Inorganic Chemistry

Article

pubs.acs.org/IC

Striking Difference in Antiproliferative Activity of Ruthenium- and Osmium-Nitrosyl Complexes with Azole Heterocycles

Gabriel E. Büchel,[†,‡,⊥] Anatolie Gavriluta,[†,‡,⊥] Maria Novak,[†] Samuel M. Meier,[†] Michael A. Jakupec,[†] Olesea Cuzan,[§] Constantin Turta,[§] Jean-Bernard Tommasino,[‡] Erwann Jeanneau,[‡] Ghenadie Novitchi,[∥] Dominique Luneau,*[,‡] and Vladimir B. Arion*[,†]

[†]Institute of Inorganic Chemistry, University of Vienna, Währinger Strasse 42, A-1090 Vienna, Austria

[‡]Laboratoire des Multimatériaux et Interfaces (UMR5615), Université Claude Bernard Lyon 1, Campus de La Doua, 69622 Villeurbanne, Cedex, France

[§]Institute of Chemistry, Academy of Sciences of Moldova, Academiei Str. 3, MD-2028 Chisinau, Moldova

[∥]Laboratoire National des Champs Magnétiques Intenses-CNRS, Université Joseph Fourier, 25 Avenue des Martyrs, 38042 Grenoble Cedex 9, France

Supporting Information

ABSTRACT: Ruthenium nitrosyl complexes of the general formulas (cation)$^+$[*cis*-$RuCl_4(NO)$(Hazole)]$^-$, where (cation)$^+$ = $(H_2ind)^+$, Hazole = 1*H*-indazole (Hind) (**1c**), (cation)$^+$ = $(H_2pz)^+$, Hazole = 1*H*-pyrazole (Hpz) (**2c**), (cation)$^+$ = $(H_2bzim)^+$, Hazole = 1*H*-benzimidazole (Hbzim) (**3c**), (cation)$^+$ = $(H_2im)^+$, Hazole = 1*H*-imidazole (Him) (**4c**) and (cation)$^+$[*trans*-$RuCl_4(NO)$(Hazole)]$^-$, where (cation)$^+$ = $(H_2ind)^+$, Hazole = 1*H*-indazole (**1t**), (cation)$^+$ = $(H_2pz)^+$, Hazole = 1*H*-pyrazole (**2t**), as well as osmium analogues of the general formulas (cation)$^+$[*cis*-$OsCl_4(NO)$(Hazole)]$^-$, where (cation)$^+$ = $(n\text{-}Bu_4N)^+$, Hazole =1*H*-indazole (**5c**), 1*H*-pyrazole (**6c**), 1*H*-benzimidazole (**7c**), 1*H*-imidazole (**8c**), (cation)$^+$ = Na^+; Hazole =1*H*-indazole (**9c**), 1*H*-benzimidazole (**10c**), (cation)$^+$ = $(H_2ind)^+$, Hazole = 1*H*-indazole (**11c**), (cation)$^+$ = H_2pz^+, Hazole = 1*H*-pyrazole (**12c**), (cation)$^+$ = $(H_2im)^+$, Hazole = 1*H*-imidazole (**13c**), and (cation)$^+$[*trans*-$OsCl_4(NO)$-(Hazole)]$^-$, where (cation)$^+$ = $n\text{-}Bu_4N^+$, Hazole = 1*H*-indazole (**5t**), 1*H*-pyrazole (**6t**), (cation)$^+$ = Na^+, Hazole = 1*H*-indazole (**9t**), (cation)$^+$ = $(H_2ind)^+$, Hazole = 1*H*-indazole (**11t**), (cation)$^+$ = $(H_2pz)^+$, Hazole = 1*H*-pyrazole (**12t**), have been synthesized. The compounds have been comprehensively characterized by elemental analysis, ESI mass spectrometry, spectroscopic techniques (IR, UV−vis, 1D and 2D NMR) and X-ray crystallography (**1c**·$CHCl_3$, **1t**·$CHCl_3$, **2t**, **3c**, **6c**, **6t**, **8c**). The antiproliferative activity of water-soluble compounds (**1c**, **1t**, **3c**, **4c** and **9c**, **9t**, **10c**, **11c**, **11t**, **12c**, **12t**, **13c**) in the human cancer cell lines A549 (nonsmall cell lung carcinoma), CH1 (ovarian carcinoma), and SW480 (colon adenocarcinoma) has been assayed. The effects of metal (Ru vs Os), cis/trans isomerism, and azole heterocycle identity on cytotoxic potency and cell line selectivity have been elucidated. Ruthenium complexes (**1c**, **1t**, **3c**, and **4c**) yielded IC_{50} values in the low micromolar concentration range. In contrast to most pairs of analogous ruthenium and osmium complexes known, they turned out to be considerably more cytotoxic than chemically related osmium complexes (**9c**, **9t**, **10c**, **11c**, **11t**, **12c**, **12t**, **13c**). The IC_{50} values of Os/Ru homologs differ by factors (Os/Ru) of up to ∼110 and ∼410 in CH1 and SW480 cells, respectively. ESI-MS studies revealed that ascorbic acid may activate the ruthenium complexes leading to hydrolysis of one M−Cl bond, whereas the osmium analogues tend to be inert. The interaction with myoglobin suggests nonselective adduct formation; i.e., proteins may act as carriers for these compounds.

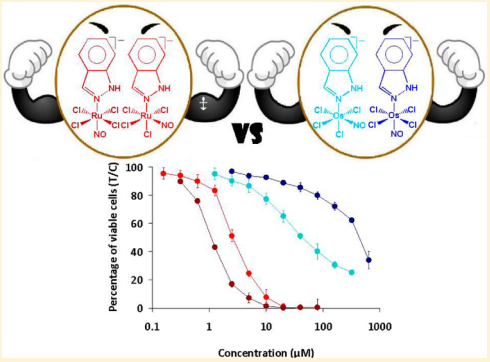

INTRODUCTION

Ruthenium nitrosyl complexes have been of interest to researchers since 1965.[1] Numerous compounds have been prepared with the aims of studying the structure and bonding in ruthenium complexes with noninnocent NO ligand,[2] investigating novel reactivities,[3] and, in particular, considering them as potential precursors for the synthesis of N_2 complexes,[3a] as models for the investigation of the elementary key steps in the global biogeochemical nitrogen cycle.[4] Other aspects of biological, medicinal, and environmental applications emphasizing the significance of ruthenium nitrosyl compounds have been subjects of reviews,[3d,5] as have their use as catalysts or catalyst precursors in a number of organic reactions.[5,6]

Ruthenium and osmium classic coordination compounds, as well as organoruthenium(II) and organoosmium(II) complexes, are subjects of current investigation as promising anticancer drug candidates.[7,8] Two most prominent investiga-

Received: March 5, 2013
Published: May 9, 2013

   dx.doi.org/10.1021/ic400555k | *Inorg. Chem.* 2013, 52, 6273−6285

Chart 1. Compounds Reported in This Work

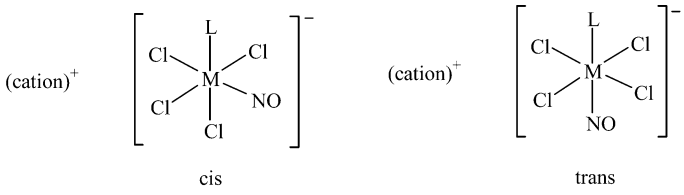

1*H*-indazole (Hind)

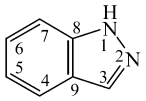

1*H*-pyrazole (Hpz)

1*H*-benzimidazole (Hbzim)

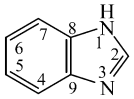

1*H*-imidazole (Him)

n-Tetrabutylammonium[b] = *n*-(Bu_4N) = ($(CH_3^D\text{-}CH_2^C\text{-}CH_2^B\text{-}CH_2^A)_4N^+$)

M	L	config	(cation)+	comp[a]
Ru	Hind	cis	H_2ind^+	**1c**
Ru	Hind	trans	H_2ind^+	**1t**
Ru	Hpz	cis	H_2pz^+	**2c**
Ru	Hpz	trans	H_2pz^+	**2t**
Ru	Hbzim	cis	H_2bzim^+	**3c**
Ru	Him	cis	H_2im^+	**4c**
Os	Hind	cis	Bu_4N^+	**5c**
Os	Hind	trans	Bu_4N^+	**5t**
Os	Hpz	cis	Bu_4N^+	**6c**
Os	Hpz	trans	Bu_4N^+	**6t**
Os	Hbzim	cis	Bu_4N^+	**7c**
Os	Him	cis	Bu_4N^+	**8c**
Os	Hind	cis	Na^+	**9c**
Os	Hind	trans	Na^+	**9t**
Os	Hbzim	cis	Na^+	**10c**
Os	Hind	cis	H_2ind^+	**11c**
Os	Hind	trans	H_2ind^+	**11t**
Os	Hpz	cis	H_2pz^+	**12c**
Os	Hpz	trans	H_2pz^+	**12t**
Os	Him	cis	H_2im^+	**13c**

[a]Underlined compounds have been studied by X-ray crystallography. [b]Atom labeling was introduced for assignments of resonances in NMR spectra.

tional drugs, namely (H_2ind)[*trans*-$Ru^{III}Cl_4(Hind)_2$], where Hind = 1*H*-indazole, (KP1019)[9] and (H_2im)[*trans*-$Ru^{III}Cl_4$(DMSO)(Him)], where Him = imidazole, (NAMI-A),[10] are currently in phase I–II clinical trials. The prodrug *trans*-$[Ru^{III}Cl_4(Hind)_2]^-$ is active as an anticancer agent in preclinical models of colon cancer and other malignancies[11] as well as in the clinical setting in refractory solid tumors including metastatic disease.[9] Although the antitumor activity of this compound was reported about 20 years ago, the mechanism of action remains unclear at least at the molecular level, and the identification of its active species is of major interest. Recently, it was reported that the combined antiangiogenic and anti-invasive properties of NAMI-A are attributed to a NO capturing mechanism responsible for metastasis control of this investigational drug.[12] The high affinity of ruthenium to NO is well-documented in the literature.[13] The pronounced effect on angiogenesis of NAMI-A was confirmed in the chick allantoic membrane and in the eye cornea model in the rabbit.[14,15] It should also be noted that NO, which is produced by a number of nitric oxide synthase (NOS) enzymes from L-arginine in the body,[16] plays a major role as a signaling molecule in biological signal transducing systems, e.g., in blood pressure regulation,[17,18] neurotransmission,[19,20] inflammatory response,[21,22] as well as necrosis[23] and apoptosis.[24,25] Nitric oxide is therefore essential in biological systems, but its excess as well as deficiency leads to pathologies. All this prompted us to synthesize ruthenium- and osmium-nitrosyl complexes with azole heterocycles and to test them for antiproliferative activity in human cancer cell lines.

Herein we report on the synthesis of 20 cis and trans isomers of ruthenium- and osmium-nitrosyl complexes (18 of which are new) of the general formula (cation)[MCl_4(NO)(Hazole)] (Chart 1) aiming at the study of the cis–trans effect on their spectroscopic features, as well as the effects of metal (Ru vs Os), cis/trans isomerism, azole heterocycle, and counterion identity on their antiproliferative activity.

EXPERIMENTAL SECTION

Materials. $Na_2[RuCl_5(NO)]\cdot 6H_2O$ was synthesized as just reported in the literature.[26] $RuCl_3$ and OsO_4 were purchased from Johnson Matthey. $NH_2OH\cdot HCl$, $K_2C_2O_4\cdot H_2O$, $NaNO_2$, 1*H*-indazole (Hind), 1*H*-benzimidazole (Hbzim), 1*H*-pyrazole (Hpz), and 1*H*-imidazole (Him) were from Aldrich and Acros, while $Na^{15}NO_2$ was from Cambridge Isotope Laboratories. All these chemicals were used without further purification. (H_2azole)$_2[RuCl_5(NO)]$ (Hazole = Hpz, Him, Hind, Hbzim) were prepared by heating $Na_2[RuCl_5(NO)]\cdot 6H_2O$ with the corresponding azole heterocycle in 6 M HCl. (n-$Bu_4N)_2[OsCl_5(NO)]$ was synthesized as described in the literature.[27,28] (n-Bu_4N)[*cis*-$OsCl_4$(NO)(Hind)] (**5c**) and (n-Bu_4N)[*trans*-$OsCl_4$(NO)(Hind)] (**5t**) were prepared by reaction of (n-$Bu_4N)_2[OsCl_5(NO)]$ with 1*H*-indazole and separated by fractional crystallization.[29] L(+)-Ascorbic acid was obtained from Acros, and ubiquitin (bovine erythrocytes) and myoglobin (equine heart) from

dx.doi.org/10.1021/ic400555k | Inorg. Chem. 2013, 52, 6273–6285

Sigma. The solvents for ESI-MS studies were methanol (VWR Int., HiPerSolv CHROMANORM), formic acid (Fluka), and Milli-Q water (18.2 MΩ, Synergy 185 UV Ultrapure Water System, Millipore, France).

Syntheses of Complexes. *$(H_2ind)[cis\text{-}RuCl_4(NO)(Hind)]\cdot 0.25CHCl_3$ (**1c**·0.25CHCl$_3$) and $(H_2ind)[trans\text{-}RuCl_4(NO)(Hind)]\cdot CHCl_3$ (**1t**·CHCl$_3$).* A suspension of $(H_2ind)_2[RuCl_5(NO)]$ (230 mg, 0.36 mmol) in 1-propanol (8 mL) was heated at 75 °C for 6 h. The solvent was removed *in vacuo*, and the residue was dissolved in chloroform. Fractional crystallization afforded rose crystals of trans-isomer **1t**·CHCl$_3$ (first fraction) which was filtered off, washed with diethyl ether, and dried *in vacuo*. Yield: 47 mg, 21%. The second fraction crystallized as cis-isomer **1c**·0.25CHCl$_3$ was filtered off, washed with diethyl ether, and dried *in vacuo*. Yield: 79 mg, 36%. Analytical data for **1c** follow. Anal. Calcd for $C_{14}H_{13}Cl_4N_5ORu\cdot 0.25\ CHCl_3$ (M_r = 540.01 g/mol): C, 31.69; H, 2.47; N, 12.96. Found: C, 31.64; H, 2.57; N, 13.28. ESI-MS in MeOH (negative): *m/z* 243 $[RuCl_4]^-$, 273 $[RuCl_4(NO)]^-$, 391 $[RuCl_4(NO)(Hind)]^-$. ESI-MS in MeOH (positive): *m/z* 119 $(H_2ind)^+$. MIR, $\tilde{\nu}$, cm^{-1}: 614, 649, 840, 925, 965, 999, 1091, 1125, 1150, 1175, 1214, 1237, 1278, 1358, 1379, 1435, 1475, 1513, 1582, 1629 (C═N), 1854 (NO), 2993, 3127 (NH), 3308. UV−vis (CH_3CN), λ_{max}, nm (ε, M^{-1} cm^{-1}): 258 (21 517), 294 sh (15 948), 373 sh (154), 453 (68), 539 sh (46). ^{1}H NMR (DMSO-d_6, 500.32 MHz), δ, ppm: 7.10 (t, 1H$_{5'}$, J = 7.01 Hz), 7.24 (t, 1H$_5$, J = 7.21 Hz), 7.34 (t, 1H$_{6'}$, J = 7.30 Hz), 7.49 (t, 1H$_6$, J = 7.16 Hz), 7.52 (d, 1H$_{7'}$, J = 7.45 Hz), 7.77 (d, 2H$_{4'/7}$, J = 9.61 Hz), 7.90 (d, 1H$_4$, J = 8.15 Hz), 8.06 (s, 1H$_{3'}$), 8.62 (s, 1H$_3$), 13.28 (s, 1H$_1$). ^{13}C{^{1}H} NMR (DMSO-d_6, 125.77 MHz), δ, ppm: 110.54 (C$_{7'}$), 111.62 (C$_{5'}$), 120.64 (C$_{4'/7}$), 120.94 (C$_{4'/7}$), 121.50 (C$_4$), 121.92 (C$_9$), 122.33 (C$_5$), 123.24 (C$_{9'}$), 126.35 (C$_{6'}$), 129.07 (C$_6$), 133.78 (C$_{3'}$), 137.80 (C$_3$), 140.10 (C$_8$), 141.04 (C$_{8'}$). ^{15}N NMR (DMSO-d_6, 50.68 MHz), δ, ppm: 163.44 (N$_1$). Suitable crystals for X-ray diffraction study were grown by slow evaporation of a solution of **1c** in chloroform.

$(H_2ind)[cis\text{-}RuCl_4(^{15}NO)(Hind)]$ was produced by following the same protocol as for **1c**, but starting from $Na_2[RuCl_5(^{15}NO)]\cdot 6H_2O$. IR (ATR), $\tilde{\nu}$, cm^{-1}: 3123 (NH), 1831 (^{15}NO), 1625 (C═N). ^{15}N NMR (50 MHz, DMSO-d_6), δ, ppm: 339.50 (NO).

Analytical data for **1t**·CHCl$_3$ follow. Anal. Calcd for $C_{14}H_{13}Cl_4N_5ORu\cdot CHCl_3$ (M_r = 629.54 g/mol): C, 28.62; H, 2.24; N, 11.12. Found: C, 28.83; H, 2.05; N, 10.97. ESI-MS in MeOH (negative): *m/z* 243 $[RuCl_4]^-$, 273 $[RuCl_4(NO)]^-$, 391 $[RuCl_4(NO)(Hind)]^-$. ESI-MS in MeOH (positive): *m/z* 119 $(H_2ind)^+$. MIR, $\tilde{\nu}$, cm^{-1}: 588, 615, 657, 731, 739, 861, 899, 962, 999, 1091, 1121, 1148, 1228, 1270, 1298, 1358, 1449, 1471, 1511, 1582, 1635 (C═N), 1891 (NO), 2995, 3158, 3232 (NH), 3317. UV−vis (CH_3CN), λ_{max}, nm (ε, M^{-1} cm^{-1}): 260 (21 883), 283 sh (16 175), 383 sh (99), 504 (36), 597 (19). ^{1}H NMR (DMSO-d_6, 500.32 MHz), δ, ppm: 7.10 (t, 1H$_{5'}$, J = 7.11 Hz), 7.22 (t, 1H$_5$, J = 7.21 Hz), 7.34 (t, 1H$_{6'}$, J = 7.23 Hz), 7.51 (t, 1H$_6$, J = 7.34 Hz), 7.54 (d, 1H$_{7'}$, J = 7.35 Hz), 7.76 (d, 1H$_{4'}$, J = 7.76 Hz), 7.79 (d, 1H$_7$, J = 7.75 Hz), 7.90 (d, 1H$_4$, J = 8.25 Hz), 8.07 (s, 1H$_{3'}$), 8.63 (s, 1H$_3$), 12.95 (s, 1H$_1$). ^{13}C{^{1}H} NMR (DMSO-d_6, 125.77 MHz), δ, ppm: 110.54 (C$_{7'}$), 112.13 (C$_7$), 120.64 (C$_{5'}$), 120.94 (C$_{4'}$), 121.01 (C$_9$), 121.94 (C$_4$), 122.36 (C$_5$), 123.23 (C$_{9'}$), 126.36 (C$_{6'}$), 129.40 (C$_6$), 133.78 (C$_{3'}$), 138.21 (C$_3$), 140.14 (C$_8$), 140.33 (C$_{8'}$). ^{15}N NMR (DMSO-d_6, 50.68 MHz), δ, ppm: 161.97 (N$_1$). Suitable crystals for X-ray diffraction study were grown by slow evaporation of a solution of **1t** in chloroform.

$(H_2ind)[trans\text{-}RuCl_4(^{15}NO)(Hind)]$ was produced by following the same protocol as for **1t**, but starting from $Na_2[RuCl_5(^{15}NO)]\cdot 6H_2O$. IR (ATR), $\tilde{\nu}$, cm^{-1}: 3237 (NH), 1849 (^{15}NO), 1631 (C═N). ^{15}N NMR (50 MHz, DMSO-d_6), δ, ppm: 343.49 (NO).

*$(H_2pz)[cis\text{-}RuCl_4(NO)(Hpz)]$ (**2c**) and $(H_2pz)[trans\text{-}RuCl_4(NO)(Hpz)]$ (**2t**).* A suspension of $(H_2pz)_2[RuCl_5(NO)]$ (160 mg, 0.36 mmol) in 1-propanol was heated at 80 °C for 7 h. The solvent was removed *in vacuo*, and the residue was dissolved in chloroform. The reddish product **2t** crystallizing first was obtained by slow diffusion of diethyl ether into the chloroform solution. Yield: 44 mg, 30%. The second collected fraction was a 1:1 mixture of **2c** and **2t**. Analytical data for **2c** follow: $C_6H_9Cl_4N_5ORu$ (M_r = 410.05 g/mol). ^{1}H NMR (DMSO-d_6, 500.32 MHz): δ 6.32 (s, 1H$_{4'}$), 6.50 (s, 1H$_4$), 7.69 (s, 2H$_{3',5'}$), 7.89 (s, 1H$_5$), 7.94 (s, 1H$_3$), 13.06 (s, 1H$_1$) ppm.

Analytical data for **2t** follow: $C_6H_9Cl_4N_5ORu$ (M_r = 410.05 g/mol). ESI-MS in MeOH (negative): *m/z* 341 $[RuCl_4(NO)(Hpz)]^-$. ESI-MS in MeOH (positive): *m/z* 69 $(H_2pz)^+$. ^{1}H NMR (DMSO-d_6, 500.32 MHz): δ 6.32 (s, 1H$_{4'}$), 6.43 (s, 1H$_4$), 7.69 (s, 2H$_{3',5'}$), 7.81 (s, 1H$_5$), 8.01 (s, 1H$_3$), 12.76 (s, 1H$_1$) ppm. Suitable crystals for X-ray diffraction study were grown by slow diffusion of diethyl ether into a solution of **2t** in chloroform.

*$(H_2bzim)[cis\text{-}RuCl_4(NO)(Hbzim)]$ (**3c**).* A suspension of $(H_2bzim)_2[RuCl_5(NO)]$ (200 mg, 0.36 mmol) in 1-propanol (4 mL) was heated at 75 °C for 17 h. The pale-rose precipitate was filtered off, washed with diethyl ether, and dried *in vacuo*. Yield: 128 mg, 68%. Anal. Calcd for $C_{14}H_{13}Cl_4N_5ORu$ (M_r = 510.17 g/mol): C, 32.96; H, 2.57; N, 13.72. Found: C, 32.99; H, 2.33; N, 13.38. ESI-MS in MeOH (negative): *m/z* 243 $[RuCl_4]^-$, 273 $[RuCl_4(NO)]^-$, 391 $[RuCl_4(NO)(Hbzim)]^-$. ESI-MS in MeOH (positive): *m/z* 119 $(H_2bzim)^+$. MIR, $\tilde{\nu}$, cm^{-1}: 591, 617, 721, 741, 750, 848, 936, 986, 1008, 1107, 1135, 1222, 1250, 1308, 1371, 1426, 1444, 1496, 1619, 1860 (NO), 3170. UV−vis (CH_3CN), λ_{max}, nm (ε, M^{-1} cm^{-1}): 267 (25 836), 251 (23 293), 383 sh (99), 504 (36), 597 (19). 470 (77), 551 (62). ^{1}H NMR (DMSO-d_6, 500.32 MHz), δ, ppm: 7.37 (m, 2H$_{5/6}$), 7.59 (m, 2H$_{5'/6'}$), 7.60 (m, 1H$_7$), 7.86 (m, 2H$_{4'/7'}$), 8.11 (m, 1H$_4$), 8.72 (d, 1H$_2$, J = 1.47 Hz), 9.53 (s, 1H$_{2'}$), 13.47 (s, 1H$_1$). ^{13}C{^{1}H} NMR (DMSO-d_6, 125.77 MHz), δ, ppm: 113.57 (C$_7$), 114.96 (C$_{4'/7'}$), 119.16 (C$_4$), 123.43 (C$_{6/5}$), 124.20 (C$_{5/6}$), 126.47 (C$_{5'/6'}$), 131.16 (C$_{8'/9'}$), 132.52 (C$_{8/9}$), 139.94 (C$_{8/9}$), 141.20 (C$_{8'/9'}$), 141.01 (C$_{2'}$), 147.08 (C$_2$). ^{15}N NMR (DMSO-d_6, 50.68 MHz), δ, ppm: 135.08 (N$_1$). Suitable crystals for X-ray diffraction study were grown by slow evaporation of a solution of **3c** in dichloromethane.

*$(H_2im)[cis\text{-}RuCl_4(NO)(Him)]\cdot 0.1CHCl_3$ (**4c**·0.1CHCl$_3$).* A suspension of $(H_2im)_2[RuCl_5(NO)]$ (300 mg, 0.67 mmol) in 1-propanol was heated at 75 °C for 19 h. The solvent was removed *in vacuo* and the residue dissolved in acetone. The unreacted starting material was precipitated as a rose powder by addition of chloroform to the acetone solution. The product was obtained by slow diffusion of diethyl ether into the mother liquor. Yield: 43 mg, 15%. Anal. Calcd for $C_6H_9Cl_4N_5ORu\cdot 0.1CHCl_3$ (M_r = 421.99 g/mol): C, 17.36; H, 2.17; N, 16.59. Found: C, 17.36; H, 2.02; N, 16.43. ESI-MS in MeOH (negative): *m/z* 341 $[RuCl_4(NO)(Him)]^-$. ESI-MS in MeOH (positive): *m/z* 69 $(H_2im)^+$. ^{1}H NMR (DMSO-d_6, 500.32 MHz), δ, ppm: 7.28 (s, 1H$_5$), 7.33 (s, 1H$_4$), 7.70 (s, 2H$_{4',5'}$), 8.19 (s, 1H$_2$), 9.10 (s, 1H$_{2'}$), 12.91 (s, 1H$_1$), 14.21 (s, 1H$_{1'/3'}$).

*$(Bu_4N)[cis\text{-}OsCl_4(NO)(Hpz)]$ (**6c**) and $(Bu_4N)[trans\text{-}OsCl_4(NO)(Hpz)]$ (**6t**).* A mixture of 1*H*-pyrazole (48 mg, 0.70 mmol) and $(n\text{-}Bu_4N)_2[OsCl_5(NO)]$ (410 mg, 0.46 mmol) in *n*-butanol (10 mL) was heated at 105 °C for 24 h. The solution was allowed to stand in an open beaker, and after 4 days blue crystals of the trans-isomer were isolated by filtration, washed with ethanol (2 × 3 mL) and diethyl ether (3 × 1 mL), and dried in vacuo. Yield: 92 mg, 30%. The filtrate produced red crystals of cis-isomer, which were filtered off on the next day, washed with ethanol (2 × 2 mL) and diethyl ether (2 × 1 mL), and dried in vacuo. Yield: 125 mg, 40%. Analytical data for **6c** follow. Anal. Calcd for $C_{19}H_{40}Cl_4N_4OOs$ (M_r = 672.59 g/mol): C, 33.93; H, 5.99; N, 8.33. Found: C, 34.37; H, 5.73; N, 8.16. ESI-MS in CH_3CN (negative): *m/z* 332 $[OsCl_4]^-$, 362 $[OsCl_4(NO)]^-$, 430 $[OsCl_4(NO)(Hpz)]^-$. IR, $\tilde{\nu}$, cm^{-1}: 587, 600, 688, 740, 777, 881, 1048, 1062, 1128, 1166, 1354, 1467, 1812 (NO), 2874, 2961, 3276. UV−vis (CH_3CN), λ_{max}, nm (ε, M^{-1} cm^{-1}): 328 (1164), 431 (466), 521 (393). ^{1}H NMR (DMSO-d_6, 500.13 MHz), δ, ppm: 0.93 (t, 12H$_D$, J = 7.3 Hz), 1.31 (sxt, 8H$_C$, J = 7.3 Hz), 1.57 (qui, 8H$_B$, J = 7.7 Hz), 3.16 (t, 8H, J = 8.4 Hz), 6.56 (qua, 1 H$_4$, J = 2.2 Hz), 7.91 (t, 1H$_5$, J = 1.8 Hz), 7.97 (t, 1 H$_3$, J = 1.7 Hz), 13.28 (s, 1H$_1$). ^{13}C{^{1}H} NMR (DMSO-d_6, 125.77 MHz), δ, ppm: 13.47 (C$_D$), 19.17 (C$_C$), 23.06 (C$_B$), 57.55 (C$_A$), 106.22 (C$_4$), 132.96 (C$_5$), 141.44 (C$_3$). ^{15}N NMR (DMSO-d_6, 50.69 MHz), δ, ppm: 65.6 (N from Bu_4N^+), 179.7 (N$_2$), 210.5 (d, N$_1$). Suitable crystals for X-ray diffraction study were picked manually from the reaction vessel under a microscope.

Analytical data for **6t** follow. Anal. Calcd for $C_{19}H_{40}Cl_4N_4OOs$ (M_r = 672.59 g/mol): C, 33.93; H, 5.99; N, 8.33. Found: C, 34.14; H, 5.83;

dx.doi.org/10.1021/ic400555k | Inorg. Chem. 2013, 52, 6273−6285

N, 8.21. ESI-MS in CH_3CN (negative): m/z 332 $[OsCl_4]^-$, 362 $[OsCl_4(NO)]^-$, 430 $[OsCl_4(NO)(Hpz)]^-$. IR, $\tilde{\nu}$, cm^{-1}: 576, 596, 667, 740, 771, 882, 1052, 1068, 1131, 1358, 1377, 1408, 1455, 1483, 1830 (NO), 2871, 2932, 2961, 3322. UV−vis (CH_3CN), λ_{max}, nm (ε, M^{-1} cm^{-1}): 323 (616), 431 (181), 574 (106). ^1H NMR (DMSO-d_6, 500.13 MHz), δ, ppm: 0.94 (t, $12H_D$, J = 7.3 Hz), 1.31 (sxt, $8H_C$, J = 7.3 Hz), 1.57 (qui, $8H_B$, J = 7.7 Hz), 3.16 (t, 8H, J = 8.4 Hz), 6.39 (t, $1H_4$, J = 2.4 Hz), 7.76 (d, $1H_5$, J = 2.4 Hz), 7.90 (d, $1H_3$, J = 2.2 Hz), 12.81 (s, $1H_1$). $^{13}C\{^1H\}$ NMR (DMSO-d_6, 125.77 MHz), δ, ppm: 13.46 (C_D), 19.18 (C_C), 23.03 (C_B), 57.51 (C_A), 104.94 (C_4), 131.89 (C_5),142.48 (C_3). ^{15}N NMR (DMSO-d_6, 50.69 MHz), δ, ppm: 65.6 (N from Bu_4N^+), 209.6 (d, N_1), 228.3 (N_2). Suitable crystals for X-ray diffraction study were picked manually from the reaction vessel under a microscope.

(Bu_4N)[cis-$OsCl_4$(NO)(Hbzim)] (**7c**). A mixture of 1*H*-benzimidazole (70 mg, 0.59 mmol) and (n-$Bu_4N)_2[OsCl_5(NO)]$ (350 mg, 0.39 mmol) in n-butanol (10 mL) was heated at 105 °C for 24 h. The solution was allowed to stand in an open beaker producing red crystals, which were filtered off after 4 days, washed with water/ethanol 1:2 (3 × 10 mL) and diethyl ether (3 × 5 mL), and dried in vacuo. Yield: 200 mg, 70%. Anal. Calcd for $C_{23}H_{42}Cl_4N_4OOs$ (M_r = 722.65 g/mol): C, 38.23; H, 5.86; N, 7.75. Found: C, 38.39; H, 5.62; N, 7.71. ESI-MS in CH_3CN (negative): m/z 332 $[OsCl_4]^-$, 362 $[OsCl_4(NO)]^-$, 410 $[OsCl_2(NO)(Hbzim)]^-$, 480 $[OsCl_4(NO)$-$(Hbzim)]^-$. IR, $\tilde{\nu}$, cm^{-1}: 427, 452, 622, 741, 885, 987, 1013, 1110, 1134, 1248, 1309, 1379, 1411, 1464, 1510, 1808, 2873, 2960, 3252. UV−vis (CH_3CN), λ_{max}, nm (ε, M^{-1} cm^{-1}): 270 (6490), 358 sh (444), 527 (132). ^1H NMR (DMSO-d_6, 500.13 MHz), δ, ppm: 0.93 (t, $12H_D$, J = 7.3 Hz), 1.31 (sxt, $8H_C$, J = 7.3 Hz), 1.57 (qui, $8H_B$, J = 7.7 Hz), 3.17 (t, 8H, J = 8.4 Hz), 7.37 (qui, $2H_{5,6}$, J = 8.3 Hz), 7.68 (d, $1H_7$, J = 7.2 Hz), 8.01 (d, $1H_4$, J = 8.0 Hz), 8.67 (s, $1H_2$), 13.57 (s, $1H_1$). $^{13}C\{^1H\}$ NMR (DMSO-d_6, 125.77 MHz), δ, ppm: 13.47 (C_D), 19.18 (C_C), 23.07 (C_B), 57.53 (C_A), 113.16 (C_7), 118.48 (C_4),123.00 (C_6), 123.97 (C_5), 131.90 (C_8), 140.21 (C_9), 147.48 (C_2). ^{15}N NMR (DMSO-d_6, 50.69 MHz), δ, ppm: 65.6 (N from Bu_4N^+), 137.8 (N_2), 158.0 (N_1). X-ray diffraction quality single crystals were picked manually from the reaction vessel under a microscope.

(Bu_4N)[cis-$OsCl_4$(NO)(Him)] (**8c**). A mixture of 1*H*-imidazole (60 mg, 0.88 mmol) and (n-$Bu_4N)_2[OsCl_5(NO)]$ (520 mg, 0.59 mmol) in n-butanol (10 mL) was heated at 105 °C for 24 h. The solution was allowed to stand in an open beaker producing red crystals, which were filtered after 2 days, washed with water/ethanol 1:2 (3 × 10 mL) and diethyl ether (3 × 5 mL), and dried in vacuo. Yield: 295 mg, 75%. Anal. Calcd for $C_{19}H_{40}OsCl_4N_4O$ (M_r = 672.59 g/mol): C, 33.93; H, 5.99; N, 8.33. Found: C, 34.06; H, 5.77; N, 8.30. ESI-MS in CH_3CN (negative): m/z 332 $[OsCl_4]^-$, 362 $[Os(NO)Cl_4]^-$, 430 $[Os(NO)$-$Cl_4(Him)]^-$. IR, $\tilde{\nu}$, cm^{-1}: 618, 656, 744, 837, 880, 1063, 1092, 1331, 1380, 1469, 1542, 1813 (NO), 2873, 2960, 3259. UV−vis (CH_3CN), λ_{max}, nm (ε, M^{-1} cm^{-1}): 307 (875), 344 sh (474), 509 (126). ^1H NMR (DMSO-d_6, 500.13 MHz), δ, ppm: 0.94 (t, $12H_D$, J = 7.3 Hz), 1.31 (sxt, $8H_C$, J = 7.3 Hz), 1.58 (qui, $8H_B$, J = 7.7 Hz), 3.17 (t, 8H, J = 8.4 Hz), 7.33 (ps.t, $1H_5$), 7.35 (ps.t, $1H_4$), 8.2 (ps.t, $1H_2$), 13.03 (s, $1H_1$). $^{13}C\{^1H\}$ NMR (DMSO-d_6, 125.77 MHz), δ, ppm: 13.48 (C_D), 19.19 (C_C), 23.07 (C_B), 57.54 (C_A), 116.78 (C_5), 128.87 (C_4),139.18 (C_3). ^{15}N NMR (DMSO-d_6, 50.69 MHz), δ, ppm: 65.6 (N from Bu_4N^+), 151.8 (N_2), 171.9 (N_1). Suitable crystals for X-ray diffraction study were picked manually from the reaction vessel under a microscope.

Na[cis-$OsCl_4$(NO)(Hind)]·$2H_2O$ (**9c**·$2H_2O$). To a solution of (n-Bu_4N)[*cis*-$OsCl_4$(NO)(Hind)][29] (**5c**) (200 mg, 0.27 mmol) in water/ethanol 1:1 (200 mL) was added ion exchanger Dowex Marathon C Na^+-form (25 g). The suspension was stirred for 12 h, the ion exchanger separated by filtration, and the solution lyophilized to give a red solid. Yield: 125 mg, 92%. Anal. Calcd for $C_7H_6Cl_4N_3NaOOs·2H_2O$ (M_r = 539.20 g/mol): C, 15.59; H, 1.87; N, 7.79. Found: C, 15.86; H, 1.59; N, 7.35. ESI-MS in CH_3CN (negative): m/z 332 $[OsCl_4]^-$, 362 $[OsCl_4(NO)]^-$, m/z 480 $[OsCl_4(NO)(Hind)]^-$. IR, $\tilde{\nu}$, cm^{-1}: 430, 560, 641, 746, 845, 969, 1004, 1042, 1092, 1125, 1239, 1359, 1383, 1515, 1627, 1825, 3309, 3494. UV−vis (CH_3CN), λ_{max}, nm (ε, M^{-1} cm^{-1}): 420 sh (114), 505 (83). UV−vis (H_2O), λ_{max}, nm (ε, M^{-1} cm^{-1}): 420 sh (137), 499 (123). UV−vis (DMSO), λ_{max}, nm (ε, M^{-1} cm^{-1}): 430 sh (114), 521 (107). UV−vis (DMF), λ_{max}, nm (ε, M^{-1} cm^{-1}): 430 (116), 518 (100). ^1H NMR (DMSO-d_6, 500.32 MHz), δ, ppm: 7.17 (s, $1H_6$), 7.39 (s, $1H_5$), 7.72 (d, $1H_4$, J = 8.2 Hz), 7.85 (d, $1H_7$, J = 7.3 Hz), 8.55 (s, $1H_3$), 13.47 (s, $1H_1$).

Na[trans-$OsCl_4$(NO)(Hind)]·$1.8H_2O$ (**9t**·$1.8H_2O$). To a solution of (n-Bu_4N)[*trans*-$OsCl_4$(NO)(Hind)][29] (**5t**) (200 mg, 0.27 mmol) in water/ethanol 1:1 (250 mL) was added ion exchanger Dowex Marathon C Na^+-form (25 g). The suspension was stirred for 12 h, the ion exchanger was separated by filtration, and the solution lyophilized to give a blue solid. Yield: 122 mg, 90%. Anal. Calcd for $C_7H_6Cl_4N_3NaOOs·1.8H_2O$ (M_r = 535.29 g/mol): C, 15.69; H, 1.80; N, 7.84. Found: C, 15.88; H, 1.44; N, 7.58. ESI-MS in CH_3CN (negative): m/z 332 $[OsCl_4]^-$, 362 $[OsCl_4(NO)]^-$, m/z 480 $[OsCl_4(NO)(Hind)]^-$. IR, $\tilde{\nu}$, cm^{-1}: 424, 596, 642, 744, 786, 858, 967, 1002, 1090, 1124, 1240, 1272, 1359, 1472, 1514, 1628, 1830, 3352, 3494. UV−vis (CH_3CN), λ_{max}, nm (ε, M^{-1} cm^{-1}): 420 sh (86), 484 (56), 568 (54). UV−vis (H_2O), λ_{max}, nm (ε, M^{-1} cm^{-1}): 420 (90), 478 (66), 542 (64). UV−vis (DMSO), λ_{max}, nm (ε, M^{-1} cm^{-1}): 420 sh (75), 497 (50), 572 (58). UV−vis (DMF), λ_{max}, nm (ε, M^{-1} cm^{-1}): 420 (85), 496 (59), 574 (64). ^1H NMR (DMSO-d_6, 500.32 MHz), δ, ppm: 7.23 (t, $1H_6$, J = 6.6 Hz), 7.52 (t, $1H_5$, J = 6.4 Hz), 7.75 (d, $1H_4$, J = 8.4 Hz), 7.90 (d, $1H_7$, J = 7.8 Hz), 8.58 (s, $1H_3$), 12.99 (s, $1H_1$).

Na[cis-$OsCl_4$(NO)(Hbzim)]·$0.4C_3H_6O$ (**10c**·$0.4C_3H_6O$). To a solution of **7c** (202 mg, 0.28 mmol) in water/ethanol 1:1 (250 mL) was added ion exchanger Dowex Marathon C Na^+-form (25 g). The suspension was stirred for 12 h, the ion exchanger was separated by filtration, and the solution was evaporated. The residue was dissolved in acetone. The solution generated a red product by slow evaporation. Yield: 123 mg, 92%. Anal. Calcd for $C_7H_6Cl_4N_3NaOOs·0.4C_3H_6O$ (M_r = 526.40 g/mol): C, 18.71; H, 1.61; N, 7.98. Found: C, 18.47; H, 1.78; N, 7.60. ESI-MS in CH_3CN (negative): ESI-MS in CH_3CN (negative): m/z 332 $[OsCl_4]^-$, 362 $[OsCl_4(NO)]^-$, 480 $[OsCl_4(NO)$-$(Hbzim)]^-$. IR, $\tilde{\nu}$, cm^{-1}: 421, 452, 586, 607, 666, 730, 989, 1016, 1111, 1246, 1307, 1361, 1416, 1464, 1494, 1514, 1610, 1645, 1827 (NO), 3156, 3332, 3536. UV−vis (CH_3CN), λ_{max}, nm (ε, M^{-1} cm^{-1}): 375 (217), 430 sh (162), 515 (118). UV−vis (H_2O), λ_{max}, nm (ε, M^{-1} cm^{-1}): 430 sh (128), 510 (114). ^1H NMR (DMSO-d_6, 500.32 MHz), δ, ppm: 7.32 (qui, $2H_{5,6}$, J = 6.8 Hz), 7.65 (d, $1H_7$, J = 6.5 Hz), 7.97 (d, $1H_4$, J = 7.2 Hz), 8.59 (s, $1H_2$).

(H_2ind)[cis-$OsCl_4$(NO)(Hind)] (**11c**). To 1*H*-indazole (20 mg, 0.17 mmol) in water (1.5 mL) was added 12 M hydrochloric acid (0.02 mL, 0.24 mmol). The resulting solution of indazolium chloride was then added to a solution of **9c** (70 mg, 0.13 mmol) in water (1.5 mL). The reaction mixture produced a red solid, which was filtered off, washed with water (3 × 1 mL), and dried in vacuo. Yield: 35 mg, 45%. Anal. Calcd for $C_{14}H_{13}N_5Cl_4OOs$ (M_r = 617.35 g/mol): C, 27.24; H, 2.45, N, 11.34. Found: C, 27.48; H, 2.40; N, 10.79. ESI-MS in CH_3CN (negative): m/z 332 $[OsCl_4]^-$, 362 $[OsCl_4(NO)]^-$, 378 $[OsCl_2(Hind)$ − $H]^-$, 480 $[OsCl_4(NO)(Hind)]^-$. IR, $\tilde{\nu}$, cm^{-1}: 427, 446, 536, 613, 741, 828, 968, 1003, 1092, 1125, 1150, 1187, 1247, 1304, 1357, 1378, 1431, 1513, 1584, 1629, 1813 (NO), 3126, 3492. UV−vis (CH_3CN), λ_{max}, nm (ε, M^{-1} cm^{-1}): 375 sh (236), 418 sh (172), 504 (120). UV−vis (H_2O), λ_{max}, nm (ε, M^{-1} cm^{-1}): 420 sh (140), 499 (128). ^1H NMR (DMSO-d_6, 500.32 MHz), δ, ppm: 7.10 (t, $1H_{5'}$, J = 7.1 Hz), 7.26 (t, $1H_6$, J = 7.2 Hz), 7.34 (t, $1H_{6'}$, J = 7.3 Hz), 7.49 (t, $1H_5$, J = 7.5 Hz), 7.52 (d, $1H_{7'}$, J = 7.5 Hz), 7.75 (d, $2H_{4'/4}$, J = 8.1 Hz), 7.91 (d, $1H_7$, J = 8.2 Hz), 8.07 (s, $1H_{3'}$), 8.61 (s, $1H_3$), 13.50 (s, $1H_1$).

(H_2ind)[trans-$OsCl_4$(NO)(Hind)]·$0.5H_2O$ (**11t**·$0.5H_2O$). To 1*H*-indazole (25 mg, 0.21 mmol) in water (1.7 mL) was added 12 M hydrochloric acid (0.02 mL, 0.24 mmol). The resulting solution of indazolium chloride was then added to a solution of **9t** (100 mg, 0.18 mmol) in water (1.7 mL). The reaction mixture produced a blue solid, which was filtered off, washed with water (3 × 1 mL), and dried in vacuo. Yield: 56 mg, 52%. Anal. Calcd for $C_{14}H_{13}N_5Cl_4OOs·0.5H_2O$ (M_r = 608.34 g/mol): C, 27.64; H, 2.32, N, 11.51. Found: C, 27.96; H, 2.32; N, 11.17. ESI-MS in CH_3CN (negative): m/z 332 $[OsCl_4]^-$, 362 $[OsCl_4(NO)]^-$, 378 $[OsCl_2(Hind)$ − $H]^-$, 480 $[OsCl_4(NO)$-

dx.doi.org/10.1021/ic400555k | Inorg. Chem. 2013, 52, 6273−6285

Table 1. Crystal Data and Details of Data Collection for 1c·$CHCl_3$, 1t·$CHCl_3$, 2t, and 3c

	1c·$CHCl_3$	1t·$CHCl_3$	2t	3c
empirical formula	$C_{15}H_{14}Cl_7N_5ORu$	$C_{15}H_{14}Cl_7N_5ORu$	$C_6H_9Cl_4N_5ORu$	$C_{14}H_{13}Cl_4N_5ORu$
fw	629.53	629.53	410.05	510.16
space group	$P\bar{1}$	$P\bar{1}$	$P\bar{1}$	$P2_12_12_1$
a [Å]	10.4202(8)	7.2490(7)	7.2264(2)	7.0814(4)
b [Å]	10.8557(9)	11.4371(13)	11.2833(4)	15.7409(8)
c [Å]	11.2737(9)	14.1067(18)	17.5497(6)	16.9995(9)
α [deg]	108.729(5)	68.991(5)	77.815(2)	
β [deg]	101.077(4)	89.138(5)	87.994(2)	
γ [deg]	103.425(4)	88.127(4)	77.155(2)	
V [Å^3]	1124.43(16)	1091.2(2)	1363.61(8)	1894.89(18)
Z	2	2	4	4
λ [Å]	0.710 73	0.710 73	0.710 73	0.710 73
ρ_{calcd} [g cm^{-3}]	1.859	1.916	1.923	1.788
cryst size [mm^3]	0.45 × 0.25 × 0.25	0.70 × 0.12 × 0.08	0.15 × 0.08 × 0.03	0.15 × 0.08 × 0.03
T [K]	100(2)	100(2)	100(2)	200(2)
μ [mm^{-1}]	1.547	1.594	1.923	1.404
R1[a]	0.0224	0.0338	0.0348	0.0363
wR2[b]	0.0528	0.0778	0.0635	0.0897
GOF[c]	1.094	1.023	1.012	1.018

[a] $R1 = \Sigma||F_o| - |F_c||/\Sigma|F_o|$. [b] $wR2 = \{\Sigma[w(F_o^2 - F_c^2)^2]/\Sigma[w(F_o^2)^2]\}^{1/2}$. [c] $GOF = \{\Sigma[w(F_o^2 - F_c^2)^2]/(n-p)\}^{1/2}$, where n is the number of reflections and p is the total number of parameters refined.

(Hind)]$^-$. IR, $\tilde{\nu}$, cm^{-1}: 425, 494, 538, 592, 651, 735, 787, 838, 860, 965, 1001, 1091, 1125, 1151, 1240, 1275, 1302, 1358, 1450, 1471, 1514, 1583, 1628, 1822 (NO), 2921, 3126, 3233, 3313, 3469. UV–vis (CH_3CN), λ_{max}, nm (ε, M^{-1} cm^{-1}): 360 sh (292), 424 sh (142), 490 sh (80), 570 (75). UV–vis (H_2O), λ_{max}, nm (ε, M^{-1} cm^{-1}): 420 sh (160), 475 sh (120), 540 sh (104). ^{1}H NMR (DMSO-d_6, 500.32 MHz), δ, ppm: 7.10 (t, 1H$_{5'}$, J = 7.1 Hz), 7.23 (t, 1H$_6$, J = 7.5 Hz), 7.34 (t, 1H$_{6'}$, J = 7.2 Hz), 7.52 (ps. qua, 2H$_{5/7'}$), 7.75 (ps. qua, 2H$_{4'/4}$), 7.90 (d, 1H$_7$, J = 8.1 Hz), 8.07 (s, 1H$_{3'}$), 8.57 (s, 1H$_3$), 13.00 (s, 1H$_1$).

(H_2pz)[cis-$OsCl_4$(NO)(Hpz)]·0.12C_3H_6O (**12c**·0.12C_3H_6O). To a solution of **6c** (196 mg, 0.29 mmol) in water/ethanol 1:1 (200 mL) was added ion exchanger Dowex Marathon C Na$^+$-form (25 g). The suspension was stirred for 12 h, the ion exchanger separated by filtration, and the solution was reduced in volume to 3 mL by evaporation under reduced pressure. Pyrazole (20 mg, 0.29 mmol) and 12 M HCl (0.1 mL) were added, and the mixture was stirred at room temperature for 30 min. The solution was evaporated, and the red solid was dissolved in acetone to afford the product on slow evaporation of the solution. Yield: 123 mg, 85%. Anal. Calcd for $C_6H_9N_5Cl_4OOs$·0.12C_3H_6O (M_r = 506.18 g/mol): C, 15.09; H, 1.93, N, 13.84. Found: C, 15.49; H, 1.81; N, 14.24. ESI-MS in CH_3CN (negative): m/z 332 [$OsCl_4$]$^-$, 362 [$OsCl_4$(NO)]$^-$, 430 [$OsCl_4$(NO)-(Hpz)]$^-$. IR, $\tilde{\nu}$, cm^{-1}: 572, 597, 672, 769, 887, 909, 1046, 1072, 1112, 1170, 1223, 1265, 1312, 1358, 1410, 1456, 1475, 1517, 1549, 1818 (NO), 2857, 2896, 2962, 3068, 3125. UV–vis (CH_3CN), λ_{max}, nm (ε, M^{-1} cm^{-1}): 325 sh (216), 378 (232), 502 sh (64). UV–vis (H_2O), λ_{max}, nm (ε, M^{-1} cm^{-1}): 325 (161), 378 sh (93), 420 sh (75), 502 (68). ^{1}H NMR (DMSO-d_6, 500.32 MHz), δ, ppm: 6.39 (t, 1H$_{4'}$, J = 2.0 Hz), 6.56 (qua, 1H$_4$, J = 2.2 Hz), 7.79 (d, 2H$_{3',5'}$, J = 2.0 Hz), 7.91 (s, 1H$_5$), 7.99 (s, 1H$_3$), 13.29 (s, 1H$_1$).

(H_2pz)[trans-$OsCl_4$(NO)(Hpz)] 0.4C_3H_6O (**12t**·0.4C_3H_6O). To a solution of **6t** (200 mg, 0.3 mmol) in water/ethanol 1:1 (200 mL) was added ion exchanger Dowex Marathon C Na$^+$-form (25 g). The suspension was stirred for 12 h, the ion exchanger separated by filtration, and the solution volume reduced to 5 mL. Pyrazole (20 mg, 0.3 mmol) and 12 M HCl (0.1 mL) were added to this solution, and the mixture was stirred for 30 min. The solvent was removed under reduced pressure, and the blue solid was crystallized from acetone. Yield: 130 mg, 87%. Anal. Calcd for $C_6H_9OsCl_4N_5O$·0.4C_3H_6O (M_r = 513.73 g/mol): C, 15.78; H, 2.06, N, 13.63. Found: C, 16.11; H, 1.98; N, 14.01. ESI-MS in CH_3CN (negative): m/z 332 [$OsCl_4$]$^-$, 362 [$OsCl_4$(NO)]$^-$, 430 [$OsCl_4$(NO)(Hpz)]$^-$. IR, $\tilde{\nu}$, cm^{-1}: 577, 597, 672, 764, 910, 1053, 1097, 1125, 1170, 1264, 1310, 1348, 1405, 1477, 1514, 1538, 1828 (NO), 2952, 3128, 3308. UV–vis (CH_3CN), λ_{max}, nm (ε, M^{-1} cm^{-1}): 334 (175), 425 sh (89), 475 sh (54), 580 (55). UV–vis (H_2O), λ_{max}, nm (ε, M^{-1} cm^{-1}): 330 (174), 425 (62), 475 sh (47), 560 (54). ^{1}H NMR (DMSO-d_6, 500.32 MHz): δ, ppm: 6.39 (ps.d, 1H$_{4'}$), 6.41 (ps.t, 1H$_4$), 7.77 (s, 1H$_5$), 7.81 (s, 2H$_{3',5'}$), 7.91 (s, 1H$_3$), 12.82 (s, 1H$_1$).

(H_2im)[cis-$OsCl_4$(NO)(Him)]]·0.3C_3H_6O (**13c**·0.3C_3H_6O). To a solution of **8c** (210 mg, 0.31 mmol) in water/ethanol 1:1 (200 mL) was added ion exchanger Dowex Marathon C Na$^+$-form (25 g). The suspension was stirred for 12 h, the ion exchanger separated by filtration, and the solution was evaporated under reduced pressure to a volume of ca. 4 mL. 1*H*-Imidazole (21 mg, 0.31 mmol) and 12 M HCl (0.1 mL) were added to this solution, and the mixture was stirred at room temperature for 30 min. The solvent was removed under reduced pressure, and the red solid was crystallized from acetone. Yield: 131 mg, 85%. Anal. Calcd for $C_6H_9OsN_5Cl_4O$·0.3C_3H_6O (M_r = 516.63 g/mol): C, 16.04; H, 2.10, N, 13.56. Found: C, 16.25; H, 1.92; N, 13.77. ESI-MS in CH_3CN (negative): m/z 332 [$OsCl_4$]$^-$, 362 [Os(NO)Cl_4]$^-$, 430 [Os(NO)Cl_4(Him)]$^-$. IR, $\tilde{\nu}$, cm^{-1}: 616, 646, 697, 742, 918, 1042, 1068, 1106, 1123, 1179, 1263, 1423, 1510, 1546, 1578, 1806 (NO), 2846, 2987, 3136, 3277. UV–vis (CH_3CN), λ_{max}, nm (ε, M^{-1} cm^{-1}): 368 (248), 511 (60). UV–vis (H_2O), λ_{max}, nm (ε, M^{-1} cm^{-1}): 368 sh (103), 420 sh (76), 506 (67). ^{1}H NMR (DMSO-d_6, 500.32 MHz), δ, ppm: 7.32 (qua, 1H$_5$, J = 1.5 Hz), 7.36 (qua, 1H$_4$, J = 1.2 Hz), 7.71 (d, 2H$_{4',5'}$, J = 1.3 Hz), 8.21 (qua, 1H$_2$), 9.10 (t, 1H$_{2'}$, J = 1.2 Hz), 13.02 (s, 1H$_1$), 14.31 (s, 2H$_{1',3'}$).

Physical Measurements. Elemental analyses were performed by the Microanalytical Service of the Faculty of Chemistry of the University of Vienna. MIR spectra were measured by using an ATR unit with a Perkin-Elmer 370 FTIR 2000 instrument (4000–400 cm^{-1}). FIR spectra were obtained with the same instrument in transmission mode using CsI-pellets. UV–vis spectra were recorded on a Perkin-Elmer Lambda 20 UV–vis spectrophotometer using samples dissolved in DMSO, DMF, THF, water, or methanol. The ^{1}H, ^{13}C, and ^{15}N NMR spectra were recorded at 500.32, 125.82, and 50.70 MHz on a Bruker DPX500 (Ultrashield Magnet) in DMSO-d_6. 2D ^{13}C^{1}H HSQC, ^{15}N^{1}H HSQC, ^{13}C^{1}H HMBC, and ^{1}H^{1}H COSY experiments were performed. Atom labeling with an apostrophe (Y$_x$′) was introduced for assignment of the azolium ions resonances in NMR spectra (Chart 1). Individual peaks are marked as singlet (s), doublet (d), triplet (t), quartet (qua), quintet (qui), multiplet (m),

dx.doi.org/10.1021/ic400555k | Inorg. Chem. 2013, 52, 6273–6285

Table 2. Crystal Data and Details of Data Collection for 6c, 6t, and 8c

	6c	6t	8c
empirical formula	$C_{19}H_{40}Cl_4N_4OOs$	$C_{19}H_{40}Cl_4N_4OOs$	$C_{19}H_{40}Cl_4N_4OOs$
fw	672.55	672.55	672.55
space group	$P2_1/c$	$C2/c$	$P2_1/c$
a [Å]	11.4520(10)	16.9831(5)	10.370(1)
b [Å]	13.4450(10)	17.8121(4)	19.654(2)
c [Å]	17.167(2)	19.7349(6)	14.216(1)
β [deg]	92.778(9)	111.041(3)	108.02(1)
V [Å^3]	2640.1(4)	5571.8(3)	2755.3(4)
Z	4	8	4
λ [Å]	0.71073	0.71073	0.71073
ρ_{calcd} [g cm^{-3}]	1.692	1.603	1.621
cryst size [mm^3]	0.42 × 0.24 × 0.16	0.31 × 0.18 × 0.11	0.22 × 0.20 × 0.11
T [K]	110(2)	293(2)	110(2)
μ [mm^{-1}]	5.252	4.977	5.033
R1[a]	0.0306	0.0242	0.0533
wR2[b]	0.0736	0.0614	0.1482
GOF[c]	1.087	1.004	1.031

[a] $R1 = \Sigma||F_o| - |F_c||/\Sigma|F_o|$. [b] $wR2 = \{\Sigma[w(F_o^2 - F_c^2)^2]/\Sigma[w(F_o^2)^2]\}^{1/2}$. [c] $GOF = \{\Sigma[w(F_o^2 - F_c^2)^2]/(n - p)\}^{1/2}$, where n is the number of reflections and p is the total number of parameters refined.

pseudodoublet (ps d), pseudotriplet (ps t). Electrospray ionization mass spectrometry was carried out with a Bruker Esquire$_{3000}$ instrument (Bruker Daltonics, Bremen, Germany) by using methanol as solvent. Expected and measured isotope distributions were compared. ESI-MS studies for monitoring hydrolysis and the reactivity toward biomolecules were performed on a Bruker AmaZon ion trap mass spectrometer (Bruker Daltonics GmbH, Bremen, Germany) by direct infusion at 4 μL/min using the following parameters: RF level 55%, average accumulation time 61 μs, trap drive 57.3, dry temp 180 °C, nebulizer 8 psi, dry gas 6 L/min, HV capillary +4.5 kV. For protein experiments, the samples were diluted with water/methanol/formic acid (50/50/0.1) prior to injection, and the following parameters were optimized: RF level 114%, average accumulation time 10 μs, nebulizer 6 psi, HV capillary −3.5 kV. Protein spectra were acquired over 0.5 min and averaged. Maximum entropy deconvolution was obtained by automatic data point spacing and 0.2 instrument peak width. The spectra were recorded and processed using ESI Compass 1.3 and Data Analysis 4.0 software (Bruker Daltonics GmbH, Bremen, Germany).

Crystallographic Structure Determination. X-ray diffraction measurements of ruthenium complexes were performed on a Bruker X8 APEXII CCD diffractometer, while those of osmium complexes were performed on an Oxford-Diffraction XCALIBUR, both equipped with an Oxford Cryosystem cooler device. The single crystals of **1c**·$CHCl_3$, **1t**·$CHCl_3$, **2t**, and **3c** were positioned at 35 mm from the detector, and 1866, 899, 788, and 898 frames were measured, each for 30, 20, 20, and 10 s over 1° or 2° (**3c**) scan width. The data for ruthenium complexes were processed using SAINT software.[30] The unit cell determination and data integration for osmium complexes were performed using the CrysAlis RED package.[31] Crystal data, data collection parameters, and structure refinement details are given in Tables 1 and 2. The structures were solved by direct methods and refined by full-matrix least-squares techniques. All non-hydrogen atoms were refined with anisotropic displacement parameters. H atoms were inserted in calculated positions and refined with a riding model. The following software programs and computer were used: structure solution, *SHELXS-97*; refinement, *SHELXL-97*;[32] molecular diagrams, *ORTEP-3*;[33] computer, Intel CoreDuo.

Stability in Aqueous Solutions and Reactivity Toward Ascorbic Acid, Ubiquitin, and Myoglobin. Stock solutions of complexes **1c**, **1t**, **5c**, and **5t** (200 μM), ascorbic acid (800 μM), myoglobin (100 μM), and ubiquitin (200 μM) were prepared in water. The compounds were incubated with ascorbic acid in a 1:8 molar ratio and with myoglobin/ubiquitin in a 2:1 molar ratio. The reaction mixtures containing 50 μM of the respective complex were incubated at 37 °C in the dark, and mass spectra were recorded after 0.5, 1, 3, 6, 17, 24, 72, and/or 96 h.

Inhibition of Cancer Cell Growth. Human nonsmall cell lung carcinoma (A549) and colon carcinoma cells (SW480) were provided by Brigitte Marian, Institute of Cancer Research, Department of Medicine I, Medical University of Vienna, Austria. Human ovarian carcinoma cells (CH1) were provided by Lloyd R. Kelland, CRC Centre for Cancer Therapeutics, Institute of Cancer Research, Sutton, U.K.

Cells were grown as adherent cultures in 75 cm^2 flasks (Iwaki) in Minimal Essential Medium supplemented with 10% heat-inactivated fetal bovine serum, 1 mM sodium pyruvate, 1% nonessential amino acids (from 100× ready-to-use stock), and 4 mM L-glutamine (all purchased from Sigma-Aldrich Austria) without antibiotics at 37 °C under a moist atmosphere containing 5% CO_2 and 95% air.

Cytotoxicity was determined by the MTT assay (MTT = 3-(4,5-dimethyl-2-thiazolyl)-2,5-diphenyl-2*H*-tetrazolium bromide). For this purpose, cells were harvested from culture flasks by trypsinization and seeded in aliquots of 100 μL/well into 96-well microculture plates (Iwaki) in the following cell densities to ensure exponential growth of untreated controls: 2.7 × 10^3 (A549), 0.9 × 10^3 (CH1), and 2.3 × 10^3 (SW480) cells/well. Cells were allowed to settle for 24 h and then exposed to the test compounds by addition of 100 μL/well aliquots of appropriate dilutions in culture medium. After exposure for 96 h, the medium was replaced with 100 μL/well of a 1:6 mixture of MTT solution (5 mg MTT reagent per ml phosphate-buffered saline) and RPMI 1640 medium. The medium/MTT mixture was replaced after 4 h with 150 μL/well DMSO to dissolve the formazan product formed by viable cells. Optical densities at 550 nm (corrected for unspecific absorbance at 690 nm) were measured with a microplate reader (Tecan Spectra Classic) to yield relative quantities of viable cells. The 50% inhibitory concentrations (IC_{50}) were calculated by interpolation. Evaluation is based on at least three independent experiments, except for cases of inactivity, which were tested only twice.

RESULTS AND DISCUSSION

Synthesis and Characterization of the Complexes. Taking into account our previous experience in carrying out chemical transformations by exploring Anderson rearrangements,[34] complexes **1c**, **1t**, **2c**, **2t**, **3c**, and **4c** were synthesized by heating $(H_2azole)_2[RuCl_5(NO)]$, where Hazole = 1*H*-indazole, 1*H*-pyrazole, 1*H*-benzimidazole, 1*H*-imidazole in 1-propanol at 70−75 °C for 6−17 h. Separation of cis- and trans-

dx.doi.org/10.1021/ic400555k | Inorg. Chem. 2013, 52, 6273−6285

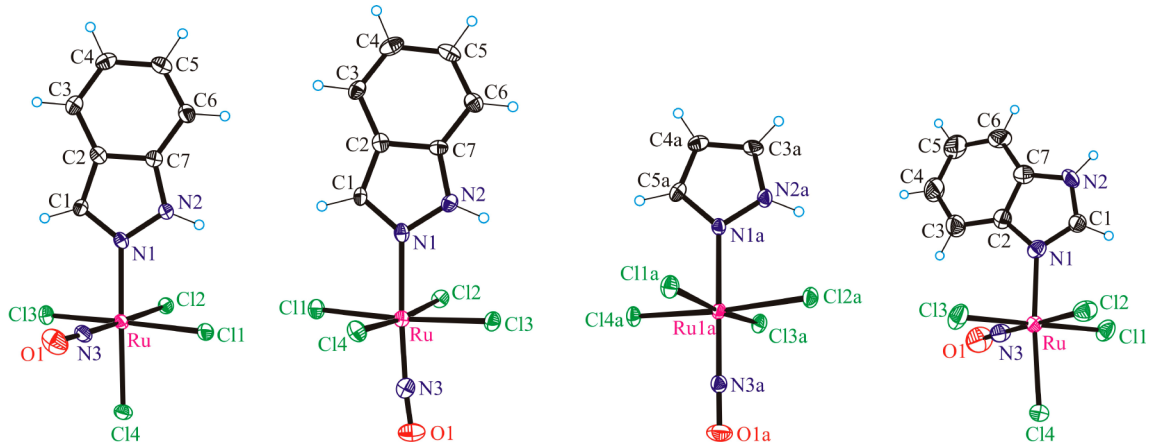

Figure 1. ORTEP views of the *cis*-$[RuCl_4(NO)(Hind)]^-$, *trans*-$[RuCl_4(NO)(Hind)]^-$, *trans*-$[RuCl_4(NO)(Hpz)]^-$, and *cis*-$[RuCl_4(NO)(Hbzim)]^-$ complex anions in **1c**, **1t**, **2t**, and **3c** (from left to right); thermal ellipsoids are drawn at 50% probability level.

Table 3. Selected Bond Distances (Å) and Angles (deg) in 1c·$CHCl_3$, 1t·$CHCl_3$, 2t, and 3c

bond	1c·$CHCl_3$	1t·$CHCl_3$	2t	3c
Ru–N1	2.073(2)	2.104(3)	2.094(2), 2.088(2)	2.068(4)
Ru–Cl_{eq}(av)	2.368(14)	2.376(6)	2.361(10), 2.363(6)	2.363(20)
Ru–Cl_{ax}	2.3672(6)			2.3893(13)
Ru–N3	1.728(2)	1.730(3)	1.727(2), 1.726(2)	1.733(5)
N3–O1	1.145(3)	1.151(3)	1.143(3), 1.147(3)	1.130(6)
Ru–N3–O1	178.2(2)	174.4(3)	175.4(2), 178.0(2)	178.0(5)

isomers of $(H_2ind)[RuCl_4(NO)(Hind)]$ (compounds **1c** and **1t**, respectively) was realized by fractional crystallization in chloroform. The less soluble trans-isomer **1t** crystallized first, and the more soluble cis-isomer **1c** thereafter. The separation of complexes **2c** and **2t** was attempted analogously. The less soluble trans-compound **2t** crystallized first. The second fraction, however, proved to be a 1:1 mixture of cis and trans complexes **2c** and **2t** as confirmed by ^{1}H NMR and X-ray crystallography. The quality of X-ray data was too poor for publication. It should be noted that the preparation of (H_2im)[*trans*-$RuCl_4(Him)(NO)$] starting from (H_2im)[*trans*-$RuCl_4$(dmso-*O*)(NO)] was reported by Alessio et al., when they studied the reactivity of NAMI-A (and analogues) toward NO.[12] Our attempts to prepare this compound by following the published procedure were not successful. However, we succeeded in synthesizing the corresponding cis-isomer **4c**. Osmium complexes **6c** and **6t** were prepared by reacting 1*H*-pyrazole with $(n\text{-}Bu_4N)_2[OsCl_5(NO)]$ in 1-butanol at 105 °C for 24 h. Fractional crystallization of the reaction mixture afforded 30% of the blue trans-isomer **6t** and then by slow evaporation of the filtrate 40% of red crystals of the cis-isomer **6c**. The reaction of 1*H*-benzimidazole and 1*H*-imidazole with $(n\text{-}Bu_4N)_2[OsCl_5(NO)]$ in 1-butanol on heating led to cis-isomers **7c** and **8c** in 70% and 75% yield, respectively. The formation of trans-isomers under these reaction conditions was negligible. To improve the aqueous solubility, to make the estimation of the toxicity caused by the tetrabutylammonium cation possible, and to elucidate structure–activity relationships, some tetrabutylammonium salts of osmium complexes were converted into the corresponding sodium and/or azolium salts. In particular, complexes **5c**, **5t**, and **7c** were treated with DOWEX Marathon C exchange resin for 12 h affording sodium salts **9c**, **9t**, and **10c** in 90–92% yield. Metathesis reactions of complexes **9c** and **9t** with indazolium chloride in water gave rise to **11c** and **11t** in 45% and 52% yield, respectively. Starting from **6c** and **6t** the corresponding sodium salts Na[*cis*-$OsCl_4(NO)(Hpz)$] and Na[*trans*-$OsCl_4(NO)(Hpz)$] prepared *in situ* were further reacted with pyrazolium chloride to give *cis*- and *trans*-$(H_2pz)[OsCl_4(NO)(Hpz)]$ (compounds **12c** and **12t**) in 85–87% yield. The formation of ruthenium- and osmium-nitrosyl complexes with azole heterocycles was confirmed by negative ion ESI mass spectra, which showed the presence of peaks attributed to $[MCl_4(NO)(Hazole)]^-$, where M = Ru, Os. All compounds possess an $S = 0$ ground state as confirmed by "normal" ^{1}H NMR spectra (without paramagnetic shift and line broadening) even at room temperature, which is in agreement with the proposed structures for compounds shown in Chart 1. Cis-isomers are characterized by lower ν(NO) wavenumbers than the trans-species. In particular, stretching vibration ν(NO) for **1c** is seen at 1854, while that of **1t** is at 1891 cm^{-1}. This vibration and the shift observed for trans-isomers relative to cis-ones ($\Delta\nu$) is markedly affected by counterion. The $\Delta\nu$ for isomers **9c** (1825 cm^{-1}) and **9t** (1830 cm^{-1}) is only 5 cm^{-1}. For pyrazole derivatives **6c** and **6t** the ν(NO) was observed at 1811 and 1830 cm^{-1}, while for related complexes **12c** and **12t** it was observed at 1818 and 1828 cm^{-1}. The ^{15}N resonances of ^{15}NO enriched isomers **1c** and **1t** are seen at 339.5 and 343.5 ppm versus solid $^{15}NH_4Cl$. The established spectroscopic differences for cis- and trans-isomers [^{1}H, ^{15}N NMR chemical shifts, ν(NO)] can serve as reliable diagnostic criteria for their identification. Note that this assignment became possible only after investigation of the isolated products by X-ray crystallography (vide infra) and correlation of their solid state structure with spectroscopic properties.

Crystal Structures. The crystal structures of **1c**·$CHCl_3$, **1t**·$CHCl_3$, **2t**, and **3c** contain essentially octahedral complexes of the general formula $[RuCl_4(NO)(Hazole)]^-$ (Figure 1). Complexes **1c**, **1t**, and **2t** crystallized in the triclinic centrosymmetric space group $P\bar{1}$, while **3c** crystallized in the

dx.doi.org/10.1021/ic400555k | *Inorg. Chem.* 2013, 52, 6273–6285

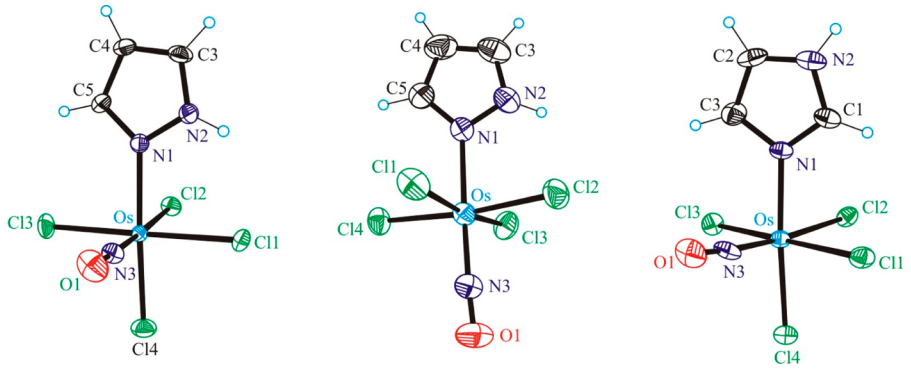

Figure 2. ORTEP views of the *cis*-$[OsCl_4(NO)(Hpz)]^-$, *trans*-$[OsCl_4(NO)(Hpz)]^-$, and *cis*-$[OsCl_4(NO)(Him)]^-$ complex anions in **6c**, **6t**, and **8c** (from left to right); thermal ellipsoids are drawn at 50%, 30%, and 50% probability levels, respectively.

orthorhombic noncentrosymmetric space group $P2_12_12_1$. The asymmetric unit of **2t**, in contrast to those of **1c**, **1t**, and **3c**, consists of two crystallographically independent complex anions, with well-comparable metric parameters. Compounds **1c** and **3c** are cis-isomers, in which three chlorido ligands and one NO molecule are bound to ruthenium in equatorial plane, and the axial sites are occupied by an azole heterocycle and fourth chlorido ligand. In trans-isomers **1t** and **2t** the equatorial plane is occupied by four chlorides, and the axial positions by NO and the azole heterocycle.

Table 3 quotes some geometrical parameters of the ruthenium coordination sphere in **1c**, **1t**, **2t**, and **3c**. It can be easily seen that Ru−N1, Ru−N3, and N3−O1 bonds in cis-isomer **1c** are significantly (6σ) shorter than in trans-isomer **1t**. In addition, the deviation from linearity of the Ru−N3−O1 bond is more pronounced in the trans-isomer than in cis.

The X-ray diffraction structures of complex anions in osmium complexes **6c**, **6t**, and **8c** are shown in Figure 2, and selected geometrical parameters can be seen in Table 4. Compounds **6c** and **8c** crystallized in the monoclinic space group $P2_1/c$, while **6t** crystallized in the monoclinic space group $C2/c$.

Table 4. Selected Bond Distances (Å) and Angles (deg) in 6c, 6t, and 8c

	6c	6t	8c
Os−N1	2.082(3)	2.116(3)	2.082(6)
Os−Cl_{eq}(av)	2.374(13)	2.368(4)	2.377(12)
Os−Cl_{ax}	2.3477(9)		2.388(2)
Os−N3	1.733(4)	1.736(4)	1.745(7)
N3−O1	1.153(4)	1.136(4)	1.155(9)
Os−N3−O1	178.1(3)	176.6(4)	173.7(6)

NMR Spectra of Ruthenium- and Osmium-Nitrosyl Complexes. ^{1}H and ^{13}C NMR spectra of compounds with azolium (**1c**, **1t**, **2c**, **2t**, **3c**, **4c**, and **11c**, **11t**, **12c**, **12t**, **13c**), sodium (**9c**, **9t**, **10c**), and *n*-Bu_4N (**6c**, **6t**, **7c**, **8c**) as countercations in DMSO-d_6 indicate that they remain intact in solution over several days at room temperature. The spectra show signals due to *n*-Bu_4N^+ or azolium cations and the coordinated azole heterocycles. The ^{1}H NMR spectra are well resolved and display identical signal sets for coordinated and metal-free azoles suggesting a diamagnetic $\{M(NO)\}^6$ configuration.

^{1}H NMR spectra of azolium cations reveal a set of split signals which is typical for a protonated azole heterocycle: two singlets for the pyrazolium cation in (**2c**, **2t**, **12c**, **12t**) at 6.31 and 7.68 ppm with relative intensities 1:2 ($1H_4'$, $2H_{3,5}'$) in accord with C_2 molecular symmetry for this cation; two triplets at 7.11 ($1H_5'$) and 7.34 ($1H_6'$) ppm, two doublets at 7.53 ($1H_7'$) and 7.75 ppm ($1H_4'$), and one singlet at 8.07 ppm ($1H_3'$) for the indazolium cation in **1c**, **1t**, **11c**, **11t**; two multiplets at 7.59 ppm ($H_{5,6}'$), 7.86 ($H_{4,7}'$) and one singlet (H_2') for the benzimidazolium cation in **3c** with relative intensities 2:2:1 in line with its C_2 symmetry; imidazolium proton signals in **4c** and **13c** appear at 7.01 ($H_{4,5'}$), 9.10 ($H_{2'}$), and 14.31 ($H_{1,3'}$) with relative intensities of 2:1:2.

Cis or trans configuration of a complex can be easily assigned by the chemical shift of the H_1 signal. The signals for cis-isomers are shifted to lower field (around 13 ppm) as compared to those for trans-complexes (around 12 ppm). The cis/trans shift difference for the signal of H_1 can be up to 1.3 ppm. We measured two-dimensional NMR spectra for compounds **1c**, **1t**, **2c**, **3c**, **6c**, **6t**, **7c**, **8c** (^{15}N,^{1}H HSQC, ^{13}C,^{1}H HSQC, ^{13}C,^{1}H HMBC, ^{1}H,^{1}H NOESY, ^{1}H,^{1}H COSY).

Indazole Compounds. The ^{1}H NMR signals of the coordinated indazole in **1c**, **1t**, **9c**, **9t**, **11c**, and **11t** show almost identical chemical shifts for all signals, except for H_1, the resonance of which appears at 13.28 (**1c**), 13.47 (**9c**), and 13.50 (**11c**) ppm for cis-compounds and 12.95 (**1t**), 12.99 (**9t**) and 13.00 (**11t**) ppm, respectively, for trans-compounds. These have been identified from ^{15}N,^{1}H HSCQ spectra (see Figures S1, S2). Another singlet for H_3 is observed at 8.6 ppm. The multiplicity of the proton resonances of coordinated indazole is the same as for the metal-free indazole. ^{1}H,^{1}H COSY spectra indicate H_4−H_5 and H_6−H_7 couplings (see Figures S3, S4). A coupling of H_3 with H_4 can be found in ^{1}H,^{13}C HMBC spectra (see Figures S5, S6). Hence, two doublets are due to H_4 (7.9 ppm) and H_7 (7.7 ppm), and two triplets can be assigned to H_5 (7.2 ppm) and H_6 (7.4 ppm). The ^{13}C{^{1}H} NMR spectra show C*H* signals for C_7, C_4, C_5, and C_6 at 112, 121, 122, and 129 ppm, correspondingly (see Figures S7, S8). C_3 is detected at 137 ppm, and two signals originating from the quaternary carbons C_8 and C_9 are at 121 and 140 ppm, respectively (see Figures S5, S6). Assignment of signals from indazole coordinated to ruthenium and osmium was performed analogously.

Benzimidazole Compounds. The ^{1}H NMR spectra of the coordinated benzimidazole in **3c**, **7c**, and **10c** show almost identical chemical shifts for all signals, except for H_1 which is seen at 13.47 (**3c**) and 13.57 ppm (**7c**), respectively (not detected in **10c**), in ^{15}N,^{1}H HSCQ spectrum (see Figure S9). Another singlet for H_2 is observed at 8.7 ppm. H_7 can be

dx.doi.org/10.1021/ic400555k | *Inorg. Chem.* 2013, 52, 6273−6285

identified from a crosspeak with H_1 in $^1H,^1H$ TOCSY. $^1H,^1H$ COSY spectrum indicates couplings of two signals from H_4 and H_7 with two overlapping signals of H_5 and H_6 with intensities 1:1:2 (see Figure S10). The $^{13}C\{^1H\}$ NMR spectrum shows CH signals for C_7, C_4, $C_{5/6}$, and $C_{5/6}$ at 113, 119, 123, and 124 ppm, correspondingly. C_2 is detected at 147 ppm, and two signals originating from the quaternary carbons C_8 and C_9 are at 132 and 139 ppm (see Figure S11). Assignment of signals from benzimidazole coordinated to ruthenium and osmium was performed analogously.

The spectroscopic (IR, NMR) data, the diamagnetic properties, and X-ray diffraction structures indicate that the monoanionic complexes $[MCl_4(NO)(Hazole)]^-$ can be described as $\{M(NO)\}^6$ systems according to the notation introduced by Feltham and Enemark, where 6 is the sum of the number of electrons in the Ru(Os) d orbitals and the number of electrons in the nitrosyl π^* orbitals.[2a]

Aqueous Solubility, Resistance to Hydrolysis, and Reactivity toward Ubiquitin and Myoglobin. The aqueous solubility of complexes **1c**, **1t**, **2c**, **2t**, **3c**, and **4c** at 298 K varies between 1.3 mM (**3c**) and 5.4 mM (**4c**), depending on the azole heterocycle identity and the countercation. The aqueous solution behavior of **1c**, **1t**, **11c**, and **11t** with respect to hydrolysis was studied by optical spectroscopy. The UV−vis

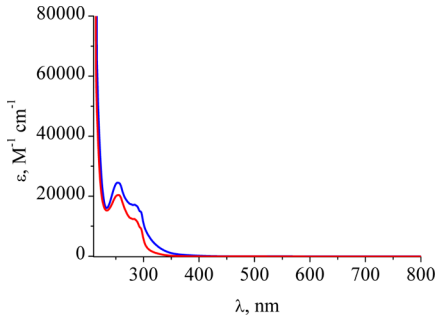

Figure 3. UV−vis spectra of aqueous solutions of $(H_2ind)[cis$-$RuCl_4(NO)(Hind)]$ (**1c**) (red trace) and $(H_2ind)[trans$-$RuCl_4(NO)(Hind)]$ (**1t**) (blue trace).

spectra of isomers **1c** and **1t** are shown in Figure 3, while their ^1H NMR spectra are in Figure 4. The complexes remain intact in aqueous solution at 294 K over at least 24 h (Ru) or 72 h (Os) (see Figures S12 and S13). Negative ion ESI-MS studies supported the findings by UV−vis experiments. The detected mass signals correspond to intact $[RuCl_4(NO)(Hind)]^-$ (m/z 391) of **1c** and **1t** and intact $[OsCl_4(NO)(Hind)]^-$ (m/z 480) of **11c** and **11t**. The latter was also observed for incubations with $(n$-$Bu_4N)[cis$-$OsCl_4(NO)(Hind)]$ (**5c**) and $(n$-$Bu_4N)[trans$-$OsCl_4(NO)(Hind)]$ (**5t**).

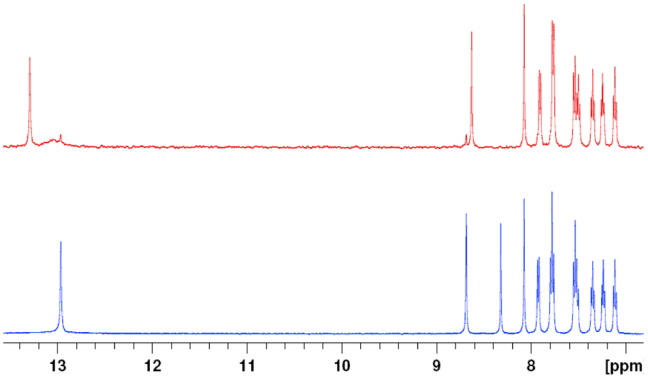

Figure 4. ^1H NMR spectra of **1c** (red trace) and **1t** (blue trace).

In addition to the parent mass signal corresponding to $[M]^-$, the complexes **1c**, **1t**, **5c**, and **5t** showed other peaks in the mass spectrum, which differ slightly for each metal. The osmium compounds **5c** and **5t** yielded $[M - (Hind)]^-$ (m/z 361.9 ± 0.1, m_{theor} = 361.83, 22 ± 6%), where M is $[cis$-$OsCl_4(NO)(Hind)]^-$ or $[trans$-$OsCl_4(NO)(Hind)]^-$. Fragments corresponding to $[M - (Hind) + H]^-$ (m/z 274.6 ± 0.1, m_{theor} = 274.78, 100%) and $[RuCl_4 + H]^-$ (m/z 245.1 ± 0.1, m_{theor} = 244.79, 25 ± 5%), where M is $[cis$-$RuCl_4(NO)(Hind)]^-$ or $[trans$-$RuCl_4(NO)(Hind)]^-$, were detected in the mass spectra of **1c** and **1t**. The mass signals due to indazole- or NO-loss were detected over the entire incubation period at constant relative intensities (Figure 5). It is therefore assumed that these signals are caused by the spraying process and not by cleavage in solution. Unlike for **5c** and **5t**, the mass signals of $[M - (Hind) + H]^-$ and $[RuCl_4 + H]^-$, where M is $[cis$-$RuCl_4(NO)(Hind)]^-$ or $[trans$-$RuCl_4(NO)(Hind)]^-$, are found at one heavier m/z-value than expected. This indicates the attachment of one proton to the fragments. In order to obtain one negative charge, the metal complex/metal ion must consequently be reduced by one electron. Hence, in the cases of the ruthenium analogues, the loss of indazole and NO in the mass spectrometer seems to be accompanied by a chemical reduction. Such a behavior was not observed for the osmium complexes. Generally, the simulated and experimental isotopic distributions match perfectly.

The unexpected redox behavior of ruthenium complexes prompted the investigation of the reactivity of both ruthenium and osmium complexes in the presence of ascorbic acid, a natural reducing agent present in every cell. Complexes **5c** and **5t** were stable in the presence of 8 equiv ascorbic acid for at least 3 days, as indicated by the presence of peaks attributed to $[M]^-$ (100%) and $[M - (Hind)]^-$ (17 ± 6%) ions, which were similarly observed when purely aqueous solutions were measured. In contrast, the mass spectra recorded upon the incubation of **1c** and **1t** with 8 equiv ascorbic acid showed complete conversion into one species within 6 h corresponding to $[M - HCl]^-$ (m/z 355.9 ± 0.1, m_{theor} = 355.85). Transient adduct formation with ascorbic acid was observed as indicated by the mass signal at $[M - Cl + Asc + H_2O]^-$ (m/z 549.9, m_{theor} = 549.89), Figure 6. Therefore, it seems that the ruthenium analogues can be activated by biological nucleophiles such as ascorbic acid leading to hydrolysis, whereas this feature was not observed for the investigated osmium compounds. The different redox behavior of the ruthenium and osmium complexes potentially provides a reason for the higher antiproliferative activity of ruthenium complexes compared to the osmium analogues.

Since the biological effect of metallodrugs may be associated with their binding to proteins, the reactivity of the four compounds was investigated toward ubiquitin (Ub) and myoglobin (Mb). The reactivity of the complexes in water and even in the presence of 8 equiv ascorbic acid yielded, however, no proof of any selective interaction in contrast to experiments with other metallodrugs.[35] The only interaction products stem from nonselective electrostatic interactions of the intact negatively-charged complexes with the positively-charged proteins (Figure S14). This suggests that serum proteins may serve as a carrier for the present metallodrugs.

dx.doi.org/10.1021/ic400555k | Inorg. Chem. 2013, 52, 6273−6285

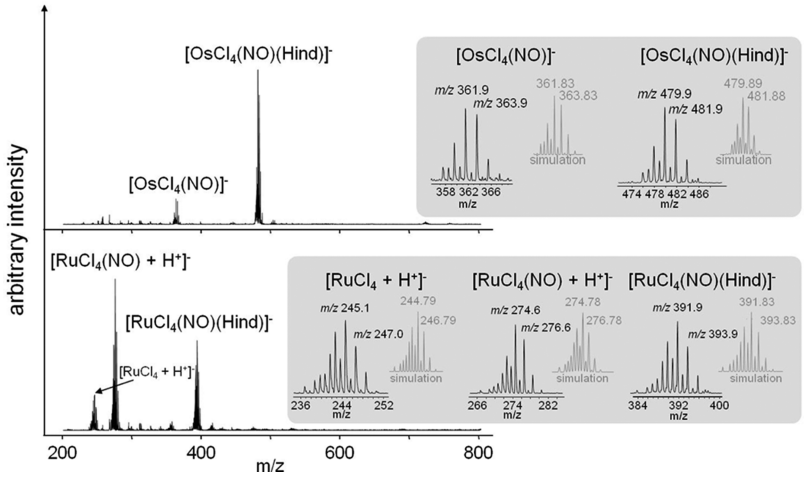

Figure 5. Full mass spectra of **1c** (bottom) and $(Bu_4N)[trans\text{-}OsCl_4(NO)(Hind)]$ (**5t**) (top) in water after 3 days. Cleavage of indazole and NO seems to occur during the spraying process. Additionally, such cleavage may result in a one-electron reduction of the metal center for **1c**. The insets show details of the metal-based mass signals and their respective simulations. All experimental values are given with STD $m/z \pm 0.1$.

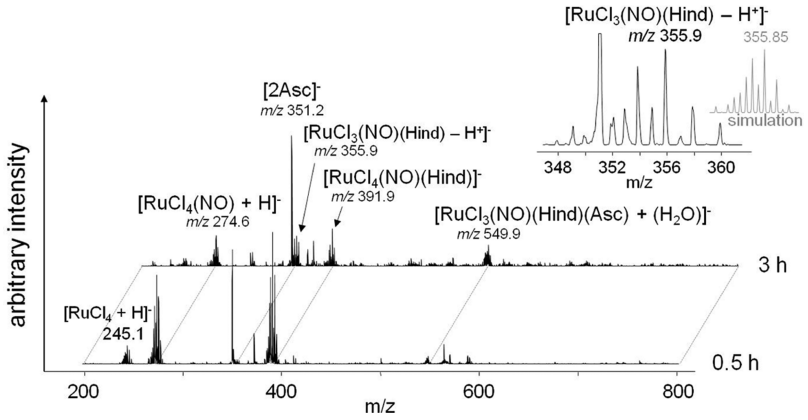

Figure 6. Mass spectra measured upon interaction between **1c** and 8 equiv ascorbic acid in aqueous solution after 0.5 and 3 h. The presence of ascorbic acid seems to lead to hydrolysis of one chlorido ligand *via* transient formation of an ascorbate adduct.

Inhibition of Cancer Cell Growth. Antiproliferative activity of novel cis- and trans-configured ruthenium- and osmium-based nitrosyl complexes with azole heterocycles was studied in the human cancer cell lines A549, CH1, and SW480. The IC_{50} values of ruthenium/osmium nitrosyl complexes are presented in Table 5. The ruthenium complexes showed similar effects in the generally more chemosensitive ovarian carcinoma cell line CH1 and the colon carcinoma cell line SW480, whereas the nonsmall cell lung cancer cell line A549 proved to be much less sensitive. On the other hand, both SW480 and A549 cells are more or less insensitive to the majority of the osmium complexes.

Overall, ruthenium complexes (**1c**, **1t**, **3c** and **4c**) yielded IC_{50} values in the low micromolar range and turned out to be much more cytotoxic than osmium complexes (**9c**, **9t**, **10c**, **11c**, **11t**, **12c**, **12t**, **13c**), which mostly require concentrations of >100 μM to exert noteworthy effects. In three specific cases, a comparison of analogues differing only in the central metal was possible (**1c** vs **11c**, **1t** vs **11t**, **4c** vs **13c**). Concentration−effect curves of these pairs of analogues are depicted in Figure 7 (for **3c**, **9c**, **9t**, **10c**, **12t**, **13c**, see Figure S15). The strongest difference was observed between trans-configured ruthenium complex **1t** (with indazole) and its osmium congener **11t**, with IC_{50} values differing by factors (Os/Ru) of ∼110 and ∼410 in CH1 and SW480 cells, respectively. A precise factor in A549

Table 5. Inhibition of Cancer Cell Growth by Compounds 1c, 1t, 3c, 4c and 9c, 9t, 10c, 11c, 11t, 12c, 12t, 13c in Three Human Cancer Cell Lines with 50% Inhibitory Concentrations (Means ± Standard Deviations), Obtained by the MTT Assay (Exposure Time: 96 h)

	IC_{50}, μM		
compd	A549	CH1	SW480
1c	14 ± 3	2.7 ± 0.6	2.6 ± 0.3
1t	8.0 ± 1.3	1.3 ± 0.3	1.1 ± 0.3
3c	7.6 ± 2.6	0.83 ± 0.17	1.8 ± 0.1
4c	35 ± 13	4.0 ± 1.1	3.7 ± 0.5
9c	>640	111 ± 45	630 ± 71
9t	>640	122 ± 14	362 ± 2
10c	>640	316 ± 57	>640
11c	128 ± 18	48 ± 13	43 ± 6
11t	>640	145 ± 12	450 ± 35
12c	>640	>640	>640
12t	>640	>640	>640
13c	>640	348 ± 112	>640
KP1019	n.d.	44 ± 11[a]	79 ± 5[a]

[a]Taken from ref 8b.

dx.doi.org/10.1021/ic400555k | *Inorg. Chem.* 2013, 52, 6273−6285

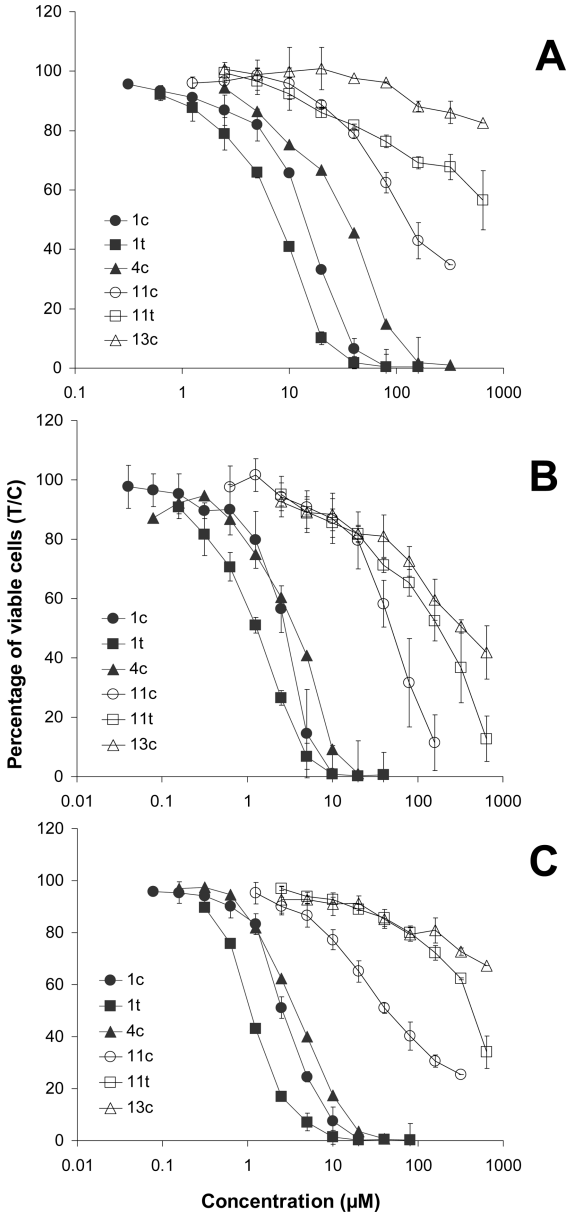

Figure 7. Concentration–effect curves of ruthenium- (**1c**, **1t**, and **4c**; filled symbols) and osmium-based analogues (**11c**, **11t**, and **13c**; unfilled symbols) in A549 (A), CH1 (B), and SW480 (C) cells, based on means ± standard deviations of at least three independent experiments each.

cells cannot be given because of the inactivity of **11t** in the concentration range tested. Even the smallest differences, those between the corresponding cis isomers **1c** and **11c**, are very pronounced, with factors of 9–18 (depending on the cell line).

The impact of cis/trans isomerism on cytotoxic potency is much smaller than that, and it is different depending on the central metal: The trans-configured ruthenium complex **1t** is about 2 times more potent than its cis analogue **1c**, based upon IC_{50} values. In contrast, the cis-configured osmium complex **11c** (with indazole) is about 3- to 10-fold more potent than its trans isomer **11t**. Alessio et al. have reported IC_{50} values in the range between 20 and 60 μM for the trans analogue of **4c** (with Ru and imidazole), which they prepared as a model compound for potential NO-containing metabolites of NAMI-A (by formal replacement of dmso with NO), but values should be compared with caution because of methodological differences. Interestingly, though, the authors obtained discouraging results in a lymphoma model in vivo, but alternatively proposed testing their compound in solid tumors under the aspect that interactions with NO might be involved in the antiangiogenic effects of NAMI-A.[10b]

The much stronger activity of ruthenium complexes is particularly remarkable, since nearly all previous comparisons of ruthenium and osmium analogues revealed either similar activities of both or higher potency of some osmium analogues.[36−47] An exception was reported for one out of three pairs of Ru(III) and Os(III) tetrazole complexes,[48] where the ruthenium species was 30 times more cytotoxic than the osmium complex. However, the difference observed in the present work is much larger. This might be caused by the contrasting hydrolytic behavior of the complexes in the presence of reductants as established by kinetic mass-spectrometric studies. Nitric oxide is a multifunctional molecule involved in a number of physiological and pathological processes. It plays a role in cellular pathways (cGMP pathway, apoptosis, and necrosis), shows activity versus DNA and heme-iron proteins (soluble guanylate cyclase, cytochrome *C* oxidase, and myoglobin), and probably can interact with the mitochondrial respiration system and induce oxidative stress.[49−52] Our results as well as those reported by others indicate that the Ru–NO bond might be more labile[53] than the Os–NO bond. Studies on the effect of ruthenium and osmium complexes on the cGMP pathway, along with investigation of their reactivity toward amino acids, are underway in our laboratory, and the results will be reported in due course.

Final Remarks. The synthesis of 18 novel ruthenium and osmium nitrosyl complexes with azole heterocycles gave a unique opportunity to study structure–cytotoxicity relationships of such type of complexes. These include water-soluble compounds with biologically relevant countercations, as well as cis and trans isomers, which have been so far unavailable. Cis- and trans-isomers can be identified by IR and NMR spectroscopy. Cis-complexes are generally characterized by lower ν(NO) wavenumbers than the trans-species; however, $\Delta\nu$ for isomeric pairs is markedly affected by counterions. The ^{15}N resonance of ^{15}NO enriched cis-isomer **1c** is upfield shifted relative to the trans-isomer **1t**, and this is appropriate for isomer identification. The effects of metal (Ru vs Os), cis/trans isomerism, and azole heterocycle identity on cytotoxic potency in the human cancer cell lines A549, CH1, and SW480 have been elucidated. An unprecedented difference in cytotoxicity for chemically related pairs of ruthenium and osmium complexes has been found. The strongest difference was observed between $(H_2ind)[trans\text{-}RuCl_4(NO)(Hind)]$ (**1t**) and $(H_2ind)[trans\text{-}OsCl_4(NO)(Hind)]$ (**11t**), with IC_{50} values differing by factors (Os/Ru) of ∼110 and ∼450 in CH1 and SW480 cells, respectively. This difference in cytotoxic activity is tentatively ascribed to the tendency of the compounds to be reduced in the biological environment. ESI-MS studies showed that **1c** and **1t** are activated in the presence of ascorbic acid leading to hydrolysis of the M–Cl bond, whereas the osmium-analogues **5c** and **5t** were inert.

■ ASSOCIATED CONTENT

Ⓢ Supporting Information

^{15}N,^{1}H HSCQ spectra of **1c**, **1t**, and **3c** (Figures S1, S2, S9); ^{1}H,^{1}H COSY spectra of **1c**, **1t**, **3c** (Figures S3, S4, S10); ^{1}H,^{13}C HMBC spectra of **1c** and **1t** (Figures S5, S6); ^{13}C,^{1}H HMBC

dx.doi.org/10.1021/ic400555k | Inorg. Chem. 2013, 52, 6273−6285

plot of **1c**, **1t**, and **3c** (Figures S7, S8, S11); UV−vis spectra of aqueous solutions of **1c** (left) and **1t** (right) (Figure S12), **11c** (left) and **11t** (right) (Figure S13); ESI MS evidence for nonselective adduct formation between myoglobin and complexes **1c**, **1t** and **5c**, **5t** (Figure S14), concentration−effect curves of complexes **3c, 9c, 9t, 10c, 12t,** and **13c** in A549 (A), CH1 (B), and SW480 (C) cells (Figure S15). Crystallographic data in CIF format. This material is available free of charge via the Internet at http://pubs.acs.org.

AUTHOR INFORMATION

Corresponding Author

*E-mail: dominique.luneau@univ-lyon1.fr (D.L.); vladimir.arion@univie.ac.at (V.B.A.).

Author Contributions

⊥These coauthors contributed equally.

Notes

The authors declare no competing financial interest.

ACKNOWLEDGMENTS

We thank Alexander Roller for collection of X-ray data sets for **1c**, **1t**, **2c**, **2t**. We are also indebted to the Austrian Science Fund (FWF) and Agence Nationale de Recherche (France) for financial support of the bilateral project I374−N19 and ANR-09-BLAN-0420-01 (VILYGRu), respectively. The PHC Amadeus and OEAD (project no. FR01/2012) are also acknowledged for their support.

REFERENCES

(1) (a) Grifith, W. P. *Adv. Organomet. Chem.* **1969**, *7*, 211−239. (b) Johnson, B. F. G.; McCleverty, J. A. *Prog. Inorg. Chem.* **1966**, *7*, 277−359. (c) Connelly, N. G. *Inorg. Chim. Acta, Rev.* **1972**, *6*, 47−89. (d) Bottomley, F. *Coord. Chem. Rev.* **1978**, *26*, 7−32.

(2) (a) Enemark, J. H.; Feltham, R. D. *Coord. Chem. Rev.* **1974**, *13*, 339−406. (b) Swinehart, J. H. *Coord. Chem. Rev.* **1967**, *2*, 385−402. (c) Eisenberg, R.; Meyer, C. D. *Acc. Chem. Res.* **1975**, *8*, 26−34.

(3) (a) McCleverty, J. A. *Chem. Rev.* **1979**, *7*, 53−76. (b) Wolak, M.; van Eldik, R. *Coord. Chem. Rev.* **2002**, *230*, 263−282. (c) Ford, P. C.; Lorkovic, I. M. *Chem. Rev.* **2002**, *102*, 993−1017. (d) Tfouni, E.; Krieger, M.; McGarvey, B. R.; Franco, D. W. *Coord. Chem. Rev.* **2003**, *236*, 57−69. (e) Videla, M.; Jacinto, J. S.; Baggio, R.; Garland, M. T.; Singh, P.; Kaim, W.; Slep, L. D.; Olabe, J. A. *Inorg. Chem.* **2006**, *45*, 8608−8617. (f) Bottomley, F.; White, P. S.; Mukaida, M.; Shimura, K.; Kakihana, H. *Dalton Trans.* **1988**, 2965−2969.

(4) (a) Hughes, M. N. In *The Inorganic Chemistry of Biological Processes*, 2nd ed.; John Wiley & Sons: New York, 1981. (b) Arikawa, Y.; Asayama, T.; Moriguchi, Y.; Agari, S.; Onishi, M. *J. Am. Chem. Soc.* **2007**, *129*, 14160−14161.

(5) McCleverty, J. A. *Chem. Rev.* **2004**, *104*, 403−418.

(6) Pandey, K. K. *Coord. Chem. Rev.* **1983**, *51*, 69−98.

(7) (a) Ang, W. H.; Dyson, P. J. *Eur. J. Inorg. Chem.* **2006**, *20*, 4003−4018. (b) Ang, W. H.; Daldini, E.; Scopelliti, R.; Juillerat-Jeannerat, L.; Dyson, P. J. *Inorg. Chem.* **2006**, *45*, 9006−9013. (c) Gossens, C.; Dorcier, A.; Dyson, P. J.; Rothlisberger, U. *Organometallics* **2007**, *26*, 3965−3975. (d) Dyson, P. J.; Sava, G. *Dalton Trans.* **2006**, 1929−1933.

(8) (a) Büchel, G. E.; Stepanenko, I. N.; Hejl, M.; Jakupec, M. A.; Arion, V. B.; Keppler, B. K. *Inorg. Chem.* **2009**, *48*, 10737−10747. (b) Büchel, G. E.; Stepanenko, I. N.; Hejl, M.; Jakupec, M. A.; Keppler, B. K.; Arion, V. B. *Inorg. Chem.* **2011**, *50*, 7690−7697. (c) Filak, L. K.; Göschl, S.; Heffeter, P.; Samper, K. G.; Egger, A. E.; Jakupec, M. A.; Keppler, B. K.; Berger, W.; Arion, V. B. *Organometallics* **2013**, *32*, 903−914.

(9) (a) Jakupec, M. A.; Arion, V. B.; Kapitza, S.; Reisner, E.; Eichinger, A.; Pongratz, M.; Marian, B.; Graf von Keyserlingk, N.; Keppler, B. K. *Int. J. Clin. Pharmacol. Ther.* **2005**, *12*, 595−596. (b) Hartinger, C. G.; Zorbas-Seifried, S.; Jakupec, M. A.; Kynast, B.; Zorbas, H.; Keppler, B. K. *J. Inorg. Biochem.* **2006**, *100*, 891−904. (c) Heffeter, P.; Böck, K.; Atil, B.; Reza Hoda, M. A.; Körner, W.; Bartel, C.; Jungwirth, U.; Keppler, B. K.; Micksche, M.; Berger, W.; Koellensperger, G. *J. Biol. Inorg. Chem.* **2010**, *15*, 737−748.

(10) (a) Rademaker-Lakhai, J. M.; van den Bongard, D.; Pluim, D.; Beijnen, J. H.; Schellens, J. H. M. *Clin. Cancer Res.* **2004**, *10*, 3717−3727. (b) Alessio, E.; Mestroni, G.; Bergamo, B.; Sava, G. *Curr. Top. Med. Chem.* **2004**, *4*, 1525−1535.

(11) Berger, M. R.; Garzon, F. T.; Keppler, B. K.; Schmähl, D. *Anticancer Res.* **1989**, *9*, 761−765.

(12) Serli, B.; Zangrado, E.; Iengo, E.; Mestroni, G.; Yellowlees, L.; Alessio, E. *Inorg. Chem.* **2002**, *41*, 4033−4043.

(13) Serli, B.; Zangrado, E.; Gianferrara, T.; Yellowlees, L.; Alessio, E. *Coord. Chem. Rev.* **2003**, *245*, 73−83.

(14) Vacca, A.; Bruno, M.; Boccarelli, A.; Coluccia, M.; Ribatti, D.; Bergamo, A.; Garbisa, S.; Sartor, L.; Sava, G. *Br. J. Cancer* **2002**, *86*, 993−998.

(15) Morbidelli, L.; Donnini, S.; Filippo, S.; Messori, L.; Piccioli, F.; Orioli, P.; Sava, G.; Ziche, M. *Br. J. Cancer* **2003**, *88*, 1484−1491.

(16) Silverman, R. B. *Acc. Chem. Res.* **2009**, *42*, 439−445.

(17) de Mel, A.; Murad, F.; Seifalian, A. M. *Chem. Rev.* **2011**, *111*, 5742−5767.

(18) Furchgott, R. F. *Angew. Chem., Int. Ed.* **1999**, *38*, 1870−1880.

(19) Garthwaite, J.; Charles, S. L.; Chess-Williams, R. *Nature* **1988**, *336*, 385−388.

(20) Dawson, T. M.; Snyder, S. H. *J. Neurosci.* **1994**, *14*, 5147−5159.

(21) Cirino, G.; Distrutti, E.; Wallace, J. L. *Inflammation Allergy: Drug Targets* **2006**, *5*, 115−119.

(22) Laroux, F. S.; Pavlick, K. P.; Hines, I. N.; Kawachi, S.; Harada, H.; Bharwani, S.; Hoffman, J. M.; Grisham, M. B. *Acta Phys. Scand.* **2001**, *173*, 113−118.

(23) Blaise, G. A.; Gauvin, D.; Gangal, M.; Authier, S. *Toxicology* **2005**, *208*, 177−192.

(24) Weigert, A.; Brüne, B. *Nitric Oxide* **2008**, *19*, 95−102.

(25) Brüne, B.; von Knethen, A.; Sandau, K. B. *Cell Death Differ.* **1999**, *6*, 969−975.

(26) Bučinský, L.; Büchel, G. E.; Ponec, R.; Rapta, P.; Breza, M.; Kožíšek, J.; Gall, M.; Biskupič, S.; Fronc, M.; Schiessl, K.; Cuzan, O.; Prodius, D.; Turta, C.; Shova, S.; Zajac, D. A.; Arion, V. B. *Eur. J. Inorg. Chem.* **2013**, DOI: 10.1002/ejic.201201526.

(27) Bhattacharya, R.; Saha, A. M.; Ghosh, P. N.; Mukherjee, M.; Mukherjee, A. K. *J. Chem. Soc., Dalton Trans.* **1991**, *3*, 501−510.

(28) Singh, P.; Sarkar, B.; Sieger, M.; Niemeyer, M.; Fiedler, J.; Zalis, S.; Kaim, W. *Inorg. Chem.* **2006**, *45*, 4602−4609.

(29) Gavriluta, A.; Büchel, G. E.; Freitag, L.; Novitchi, G.; Tommasino, J. B.; Jeanneau, E.; Kuhn, P.-S.; González, L.; Arion, V. B.; Luneau, D. *Inorg. Chem.* **2013**, DOI: 10.1021/ic4004824.

(30) *SAINT-Plus, version 7.06a and APEX2*; Bruker-Nonius AXS Inc.: Madison, WI, 2004.

(31) *CrysAlis RED, version 1.171.35.15 (release 03-08-2011 CrysAlis171.NET)*; Oxford Diffracttion Ltd., 2011.

(32) Sheldrick, G. M. *Acta Crystallogr.* **2008**, *A46*, 112−122.

(33) Burnett, M. N.; Johnson, G. K. *ORTEPIII. Report ORNL-6895*; OAK Ridge National Laboratory: Oak Ridge, TN, 1996.

(34) Davies, J. A.; Hockensmith, C. M.; Kukushkin, V. Yu.; Kukushkin, Yu. N. *Synthetic Coordination Chemistry—Principles and Practice*; World Scientific: Hackensack, NJ, 1995; pp 392−396.

(35) Meier, S. M.; Hanif, M.; Kandioller, W.; Keppler, B. K.; Hartinger, C. G. *J. Inorg. Biochem.* **2012**, *108*, 91−95.

(36) Schmid, W. F.; John, R. O.; Mühlgassner, G.; Heffeter, P.; Jakupec, M. A.; Galanski, M.; Berger, W.; Arion, V. B..; Keppler, B. K. *J. Med. Chem.* **2007**, *50*, 6343−6355.

(37) Schuecker, R.; John, R. O.; Jakupec, M. A.; Arion, V. B.; Keppler, B. K. *Organometallics* **2008**, *27*, 6587−6595.

(38) Filak, L. K.; Mühlgassner, G.; Jakupec, M. A.; Heffeter, P.; Berger, W.; Arion, V. B.; Keppler, B. K. *J. Biol. Inorg. Chem.* **2010**, *15*, 903−918.

(39) Filak, L. K.; Mühlgassner, G.; Bacher, F.; Roller, A.; Galanski, M.; Jakupec, M. A.; Keppler, B. K.; Arion, V. B. *Organometallics* **2011**, *30*, 273−283.
(40) Hanif, M.; Nazarov, A. A.; Hartinger, C. G.; Kandioller, W.; Jakupec, M. A.; Arion, V. B.; Dyson, P. J.; Keppler, B. K. *Dalton Trans.* **2010**, *39*, 7345−7352.
(41) Mühlgassner, G.; Bartel, C.; Schmid, W. F.; Jakupec, M. A.; Arion, V. B.; Keppler, B. K. *J. Inorg. Biochem.* **2012**, *116*, 180−187.
(42) Stepanenko, I. N.; Novak, M. S.; Mühlgassner, G.; Roller, A.; Hejl, M.; Arion, V. B.; Jakupec, M. A.; Keppler, B. K. *Inorg. Chem.* **2011**, *50*, 11715−11728.
(43) Cebrián-Losantos, B.; Krokhin, A. A.; Stepanenko, I. N.; Eichinger, R.; Jakupec, M. A.; Arion, V. B.; Keppler, B. K. *Inorg. Chem.* **2007**, *46*, 5023−5033.
(44) Dorcier, A.; Ang, W. H.; Bolaño, S.; Gousalvi, L.; Juillerat-Jeannerat, L.; Laurenczy, G.; Peruzzini, M.; Phillips, A. D.; Zanobini, F.; Dyson, P. J. *Organometallics* **2006**, *25*, 4090−4096.
(45) Peacock, A. F. A.; Melchart, M.; Deeth, R. J.; Habtemariam, A.; Parsons, S.; Sadler, P. J. *Chem.—Eur. J.* **2007**, *13*, 2601−2613.
(46) Peacock, A. F. A.; Habtemariam, A.; Moggach, S. A.; Prescimone, A.; Parsons, S.; Sadler, P. J. *Inorg. Chem.* **2007**, *46*, 4049−4059.
(47) Maksimoska, J.; Williams, D. S.; Atilla-Gokcumen, G. E.; Smalley, K. S. M.; Carroll, P. J.; Webster, R. D.; Filippakopoulos, P.; Knapp, S.; Meggers, E. *Chem.—Eur. J.* **2008**, *14*, 4816−4822.
(48) Stepanenko, I. N.; Krokhin, A. A.; John, R. O.; Roller, A.; Arion, V. B.; Jakupec, M. A.; Keppler, B. K. *Inorg. Chem.* **2008**, *47*, 7338−7347.
(49) Bonavida, B.; Khineche, S.; Huerta-Yepez, S.; Garbán, H. *Drug Resist. Updates* **2006**, *9*, 157−173.
(50) Brüne, B.; Knethen, A.; Sandau, K. B. *Eur. J. Pharmacol.* **1998**, *351*, 261−272.
(51) Heinrich, T. A.; Von Poelhsitz, G.; Reis, R. I.; Castellano, E. E.; Neves, A.; Lanznaster, M.; Machado, S. P.; Batista, A. A.; Costa-Neto, C. M. *Eur. J. Med. Chem.* **2011**, *46*, 3616−3622.
(52) Mocellin, S.; Bronte, V.; Nitti, D. *Med. Res. Rev.* **2007**, *27*, 317−352.
(53) Cleare, M. J. *Platinum Met. Rev.* **1968**, *12*, 131−133.